

Ab initio theoretical approaches

Noemi Rocco



NuInt, '12th International Workshop on Neutrinos-Nucleus Interactions in the Few-GeV Region'

October 15-19, 2018

In Collaboration with:

C. Barbieri (University of Surrey), O. Benhar (La Sapienza), A. Lovato (Argonne National Laboratory), V. Somà (Cea-Irfu)

Outline

GFMC

😊 Virtually exact electroweak response of nuclei $A \leq 12$, quasi elastic sector

😓 Non relativistic approximation in the kinematics and (partially) in the current operators

SCGF
CBF

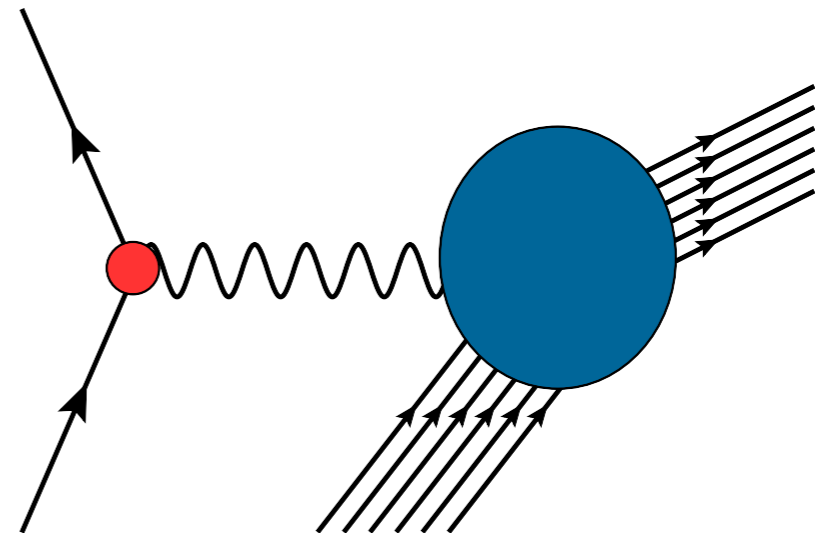
😊 Realistic Spectral Function + Impulse Approximation:
Relativistic effects accounted for, accurate description of the initial state

😓 Approximation are made in the description of hadronic final state

Lepton-nucleus scattering

The inclusive cross section of the process in which a lepton scatters off a nucleus and the hadronic final state is undetected can be written as

$$\frac{d^2\sigma}{d\Omega_\ell dE_{\ell'}} = L_{\mu\nu} W^{\mu\nu}$$



- The Leptonic tensor is fully specified by the lepton kinematic variables. For instance, in the electron-nucleus scattering case

$$L_{\mu\nu} = k_\mu k'_\nu + k'_\mu k_\nu - g_{\mu\nu} (k \cdot k') + i\epsilon_{\mu\nu\alpha\beta} k'^\alpha k^\beta$$

- The Hadronic tensor contains all the information on target response

$$W^{\mu\nu} = \sum_f \langle 0 | J^{\mu\dagger}(q) | f \rangle \langle f | J^\nu(q) | 0 \rangle \delta^{(4)}(p_0 + q - p_f)$$

Non relativistic nuclear many-body theory (NMBT) provides a fully consistent theoretical approach allowing for an accurate description of $|0\rangle$, independent of momentum transfer.

Non relativistic Nuclear Many Body Theory

- Within NMBT the nucleus is described as a collection of A point-like nucleons, the dynamics of which are described by the non relativistic Hamiltonian

$$H = \sum_i \frac{\mathbf{p}_i^2}{2m} + \sum_{i<j} v_{ij} + \sum_{i<j<k} V_{ijk} + \dots$$

The nuclear energy spectrum can be accurately determined

$$H |0\rangle = E_0 |0\rangle \quad , \quad H |f\rangle = E_f |f\rangle$$

The nuclear electromagnetic current is constrained through the continuity equation

$$\nabla \cdot \mathbf{J}_{EM} + i[H, J_{EM}^0] = 0$$

- The above equation implies that \mathbf{J}_{EM} involves two-nucleon contributions.

- Non relativistic expansion of \mathbf{J}_{EM} , in powers $|\mathbf{q}|/m$

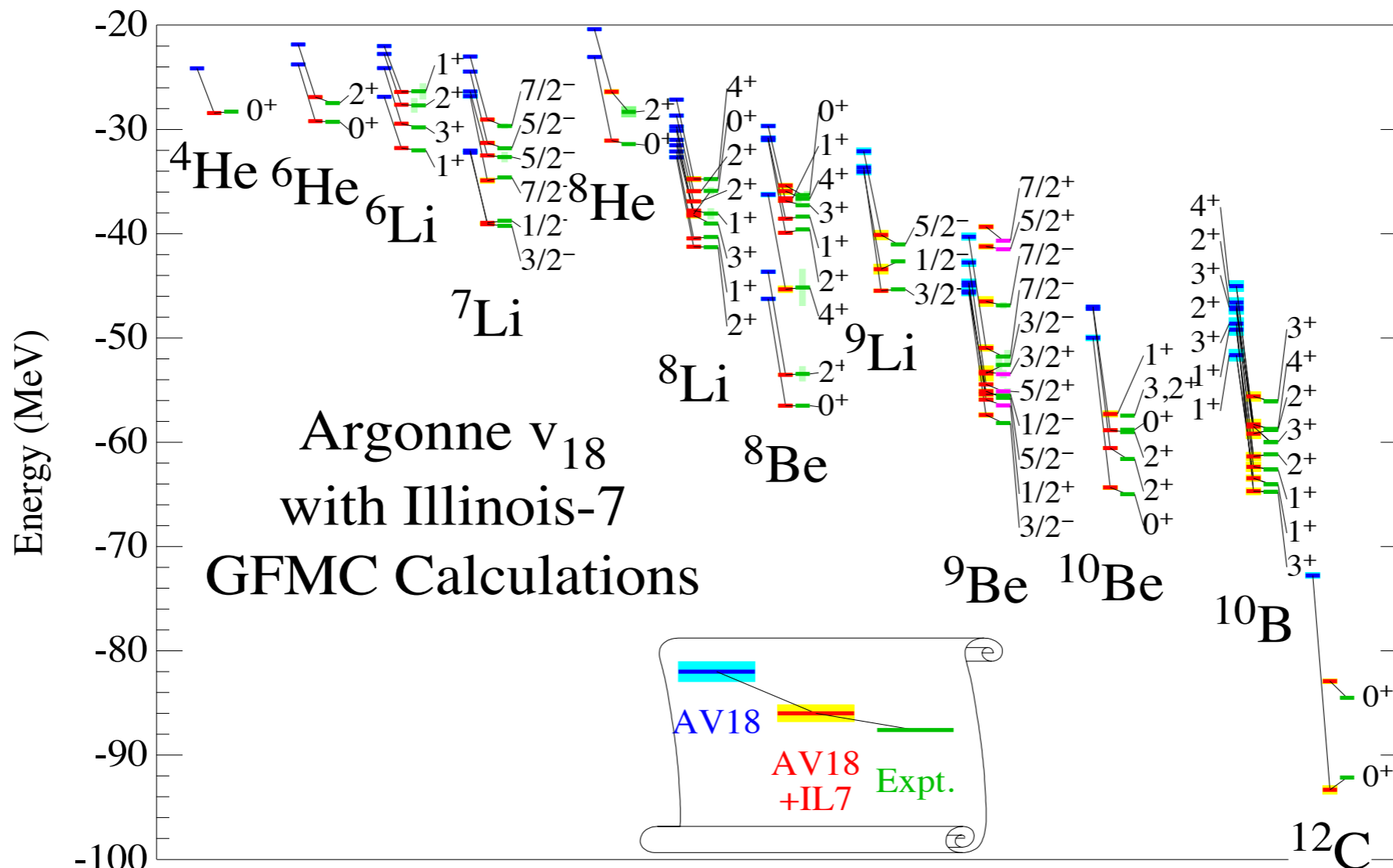


The Green's Function Monte Carlo approach

- Diffusion Monte Carlo methods use an imaginary-time projection technique to enhance the ground-state component of a starting (correlated) trial wave function.

$$\lim_{\tau \rightarrow \infty} e^{-(H-E_0)\tau} |\Psi_T\rangle = \lim_{\tau \rightarrow \infty} \sum_n c_n e^{-(E_n-E_0)\tau} |\Psi_n\rangle = c_0 |\Psi_0\rangle$$

- Suitable to solve $A \leq 12$ nuclei with $\sim 1\%$ accuracy



The Green's Function Monte Carlo approach

❖ Accurate GFMC calculations of the electroweak responses of ^4He and ^{12}C have been recently performed: [A. Lovato et al, Phys.Rev.Lett. 117 \(2016\), 082501, Phys.Rev. C97 \(2018\), 022502](#)

$$R_{\alpha\beta}(\omega, \mathbf{q}) = \sum_f \langle 0 | J_{\alpha}^{\dagger}(\mathbf{q}) | f \rangle \langle f | J_{\beta}(\mathbf{q}) | 0 \rangle \delta(\omega - E_f + E_0)$$

- Valuable information on the energy dependence of the response functions can be inferred from the their Laplace transforms

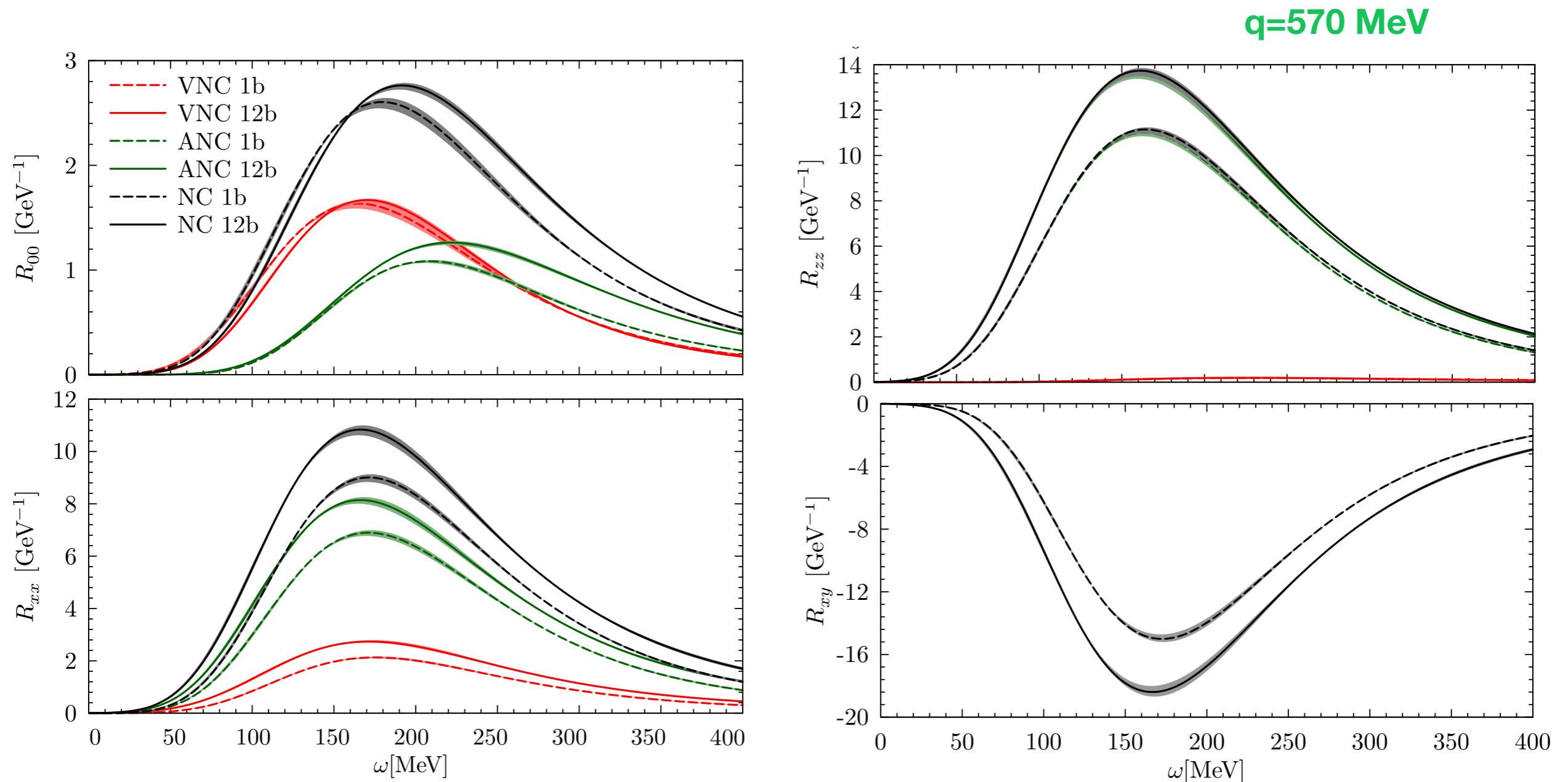
$$E_{\alpha\beta}(\mathbf{q}, \tau) = \int d\omega e^{-\omega\tau} R_{\alpha\beta}(\mathbf{q}, \omega) = \langle 0 | J_{\alpha}^{\dagger}(\mathbf{q}) e^{-(H-E_0)\tau} J_{\beta}(\mathbf{q}) | 0 \rangle$$

Using the completeness relation for the final states, we are left with ground-state expectations value

- Maximum entropy techniques are used perform the analytic continuation of the Euclidean response functions, corresponding to the “inversion” of the Laplace transforms

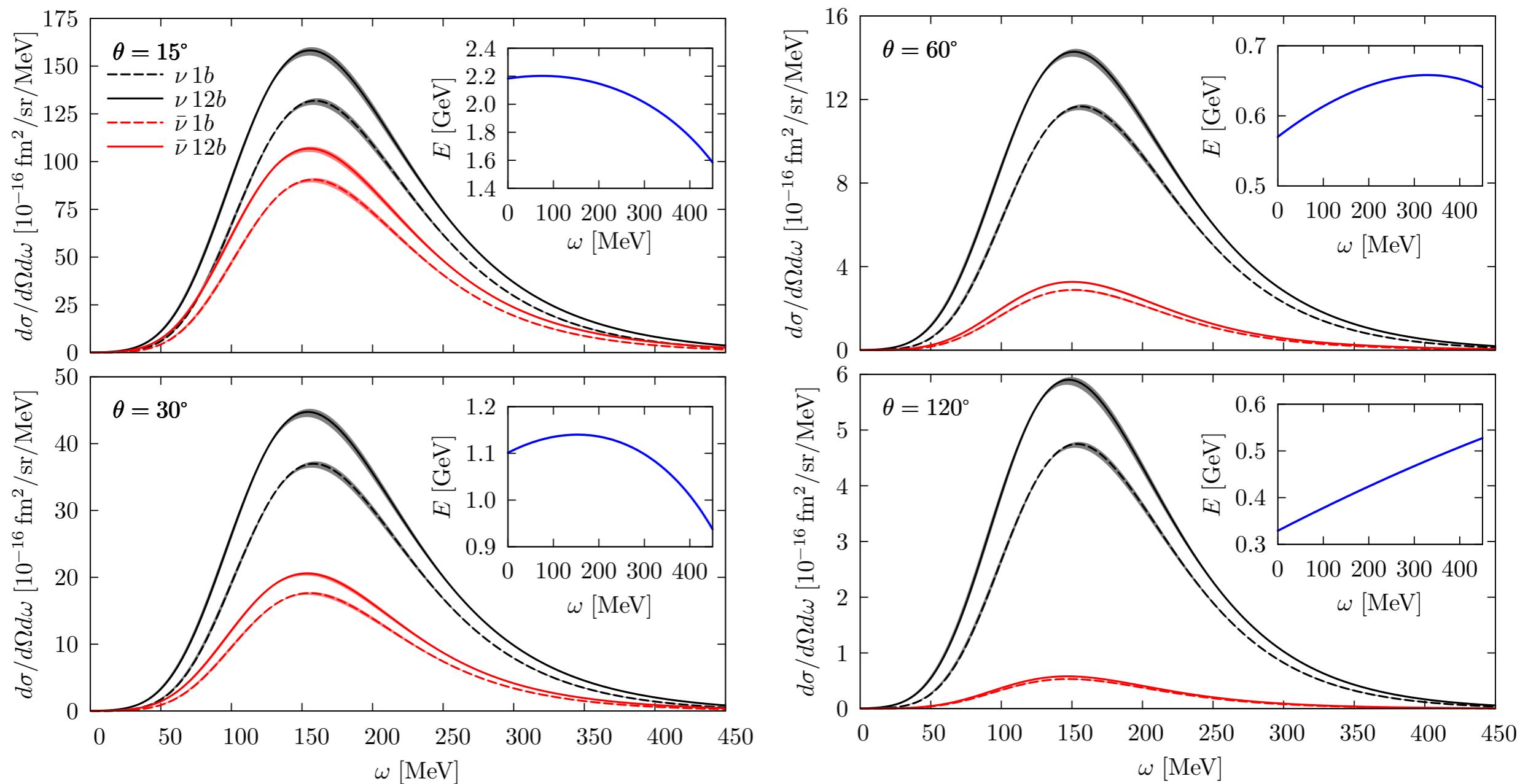
^{12}C neutral-current response

- The neutral-current response functions of ^{12}C have been recently computed



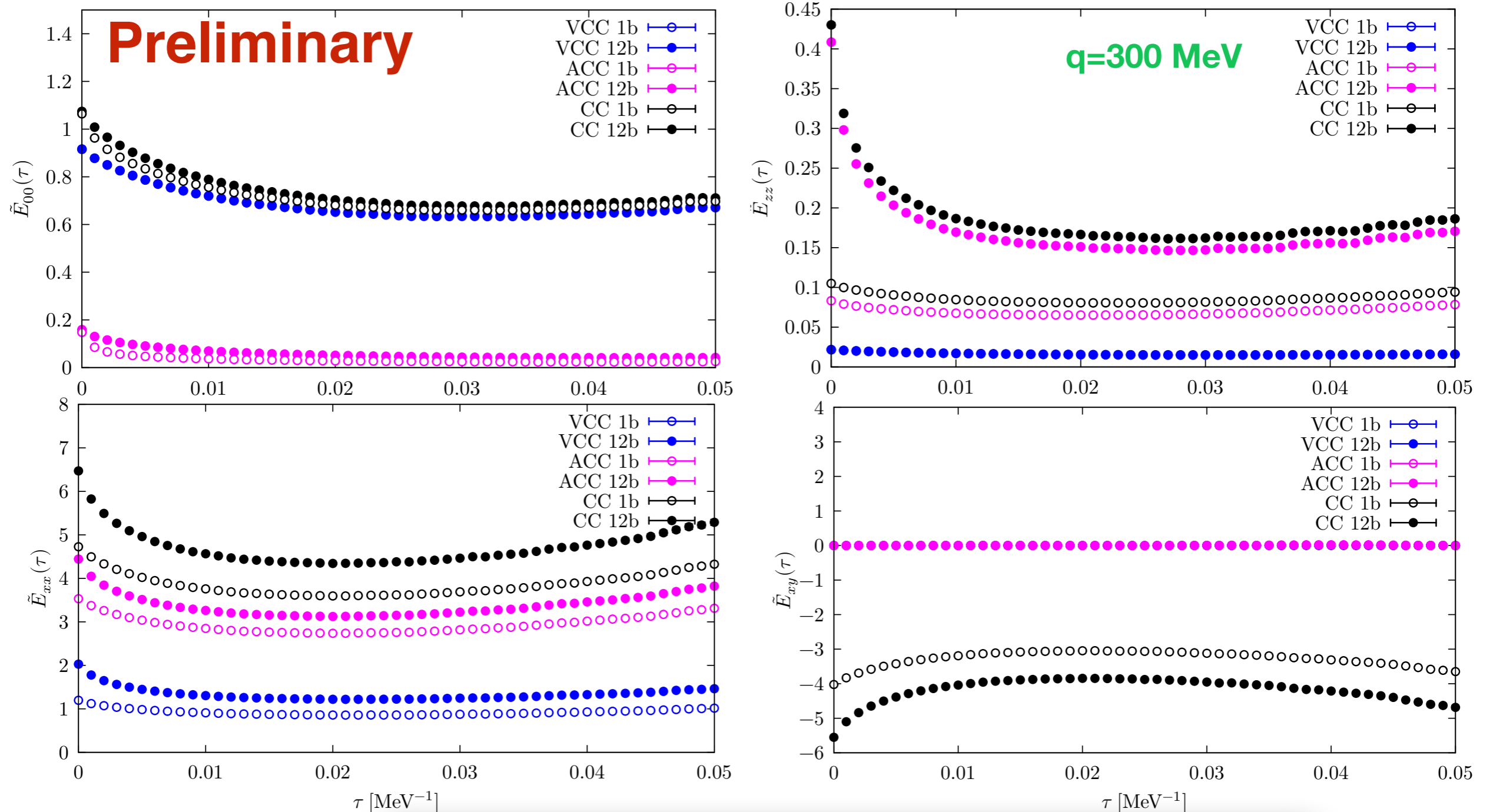
^{12}C neutral-current cross-section

- Neutrino and anti-neutrino differential cross sections for a fixed value of the three-momentum transfer as function of the energy transfer for a number of scattering angles
- The anti-neutrino cross section decreases rapidly relative to the neutrino cross section as the scattering angle changes from the forward to the backward hemisphere



^4He charge-current Euclidean responses

- The charged-current Euclidean responses of ^4He have been recently computed



The Impulse Approximation

- For sufficiently large values of $|\mathbf{q}|$, the IA can be applied under the assumptions

$$|f\rangle \longrightarrow |p\rangle \otimes |f\rangle_{A-1} \qquad J_\alpha = \sum_i j_\alpha^i$$



- The matrix element of the current can be written in the factorized form

$$\langle 0 | J_\alpha | f \rangle \longrightarrow \sum_k \langle 0 | [|k\rangle \otimes |f\rangle_{A-1}] \langle k | \sum_i j_\alpha^i | p \rangle$$

- The nuclear cross section is given in terms of the one describing the interaction with individual bound nucleons

$$d\sigma_A = \int dE d^3k d\sigma_N P(\mathbf{k}, E) \longrightarrow \frac{1}{\pi} \text{Im} G(\mathbf{k}, E)$$

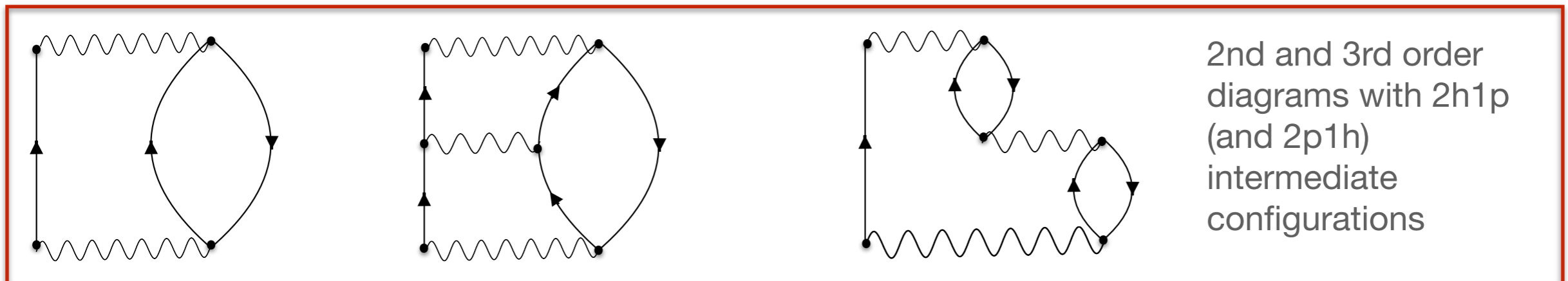
- The intrinsic properties of the nucleus are described by the hole spectral function

Self Consistent Green's Function

- Accurately solve the Dyson equation

$$\begin{array}{c} \text{---} \\ \downarrow \\ G(E) \end{array} = \begin{array}{c} \text{---} \\ \downarrow \\ G^0(E) \end{array} + \begin{array}{c} \text{---} \text{---} \\ \downarrow \\ \Sigma^*(E) \end{array}$$

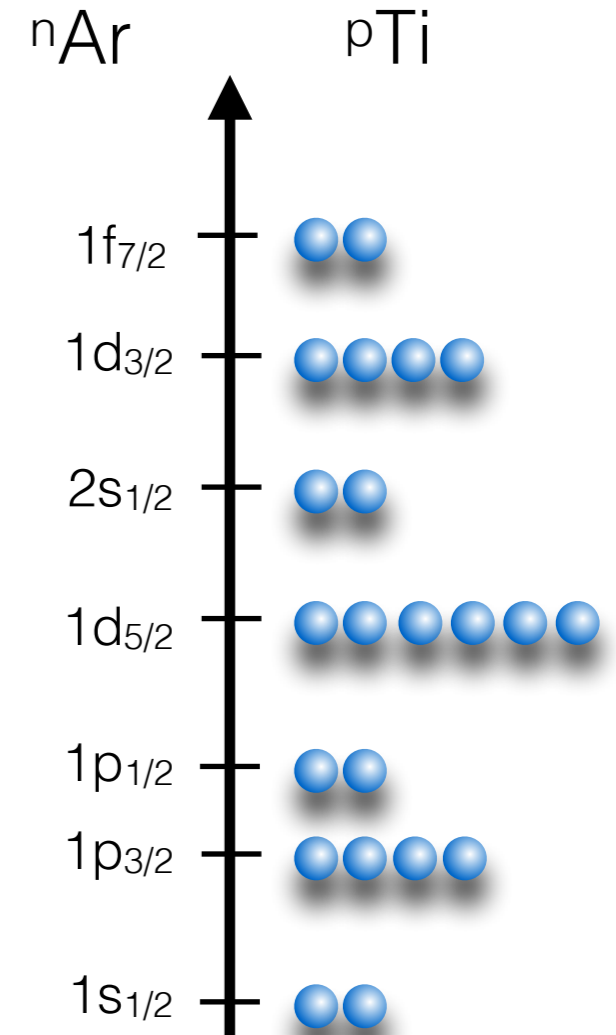
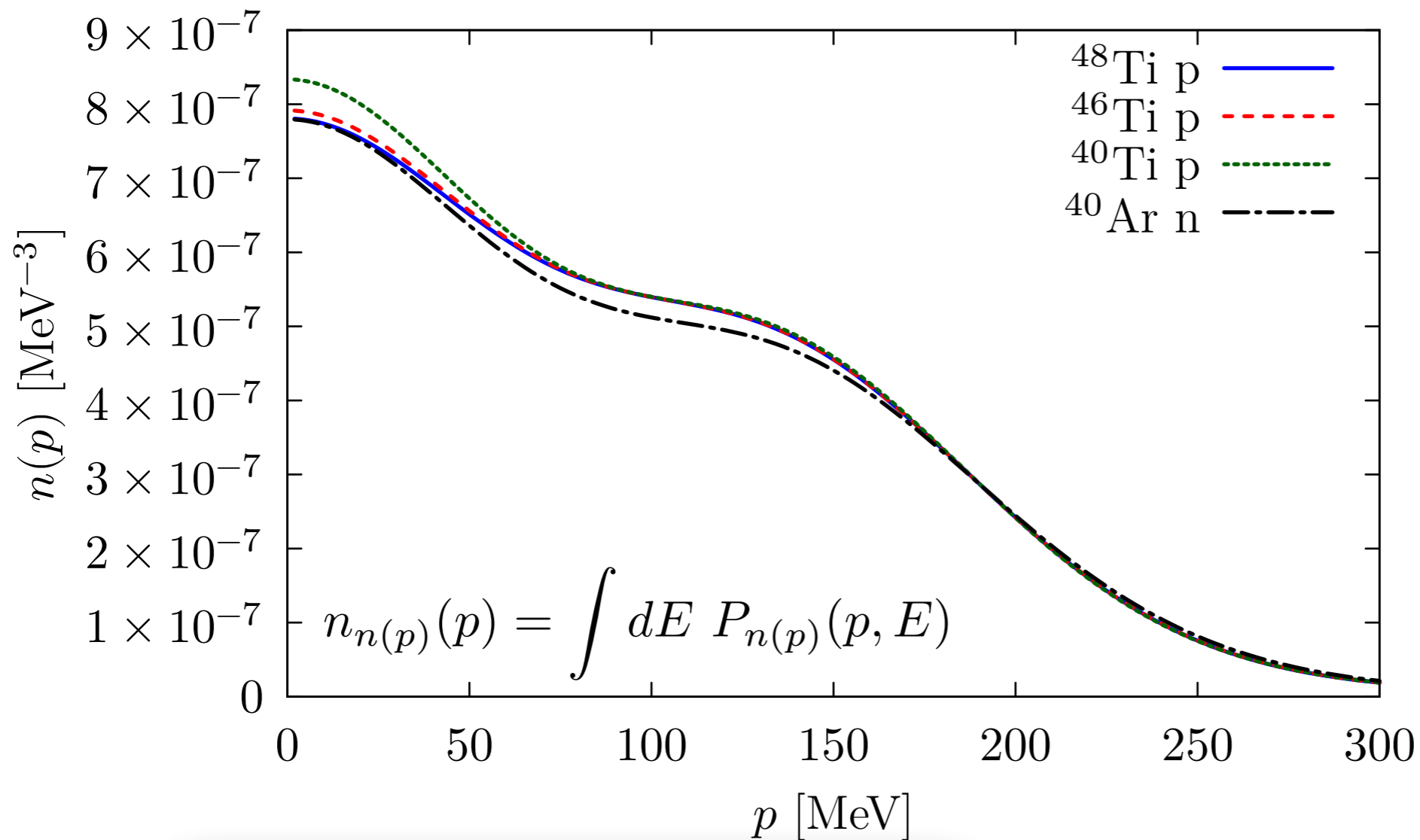
- $\Sigma^* = \Sigma^*[G(E)]$, an iterative procedure is required to solve the Dyson equation self-consistently
- The self-energy is systematically calculated in a non-perturbative fashion within the Algebraic Diagrammatic Construction (ADC). The saturating chiral interaction at NNLO (NNLO_{sat}) is used.



❖ V. Somà et al, Phys.Rev. C87 (2013) no.1, 011303 : generalization of this formalism within Gorkov theory allows to describe open-shell nuclei such as Ar⁴⁰, Ti⁴⁸ ...

Understanding the differences between mirror nuclei

- Single $n(p)$ -momentum distribution of ^{40}Ar (Ti)



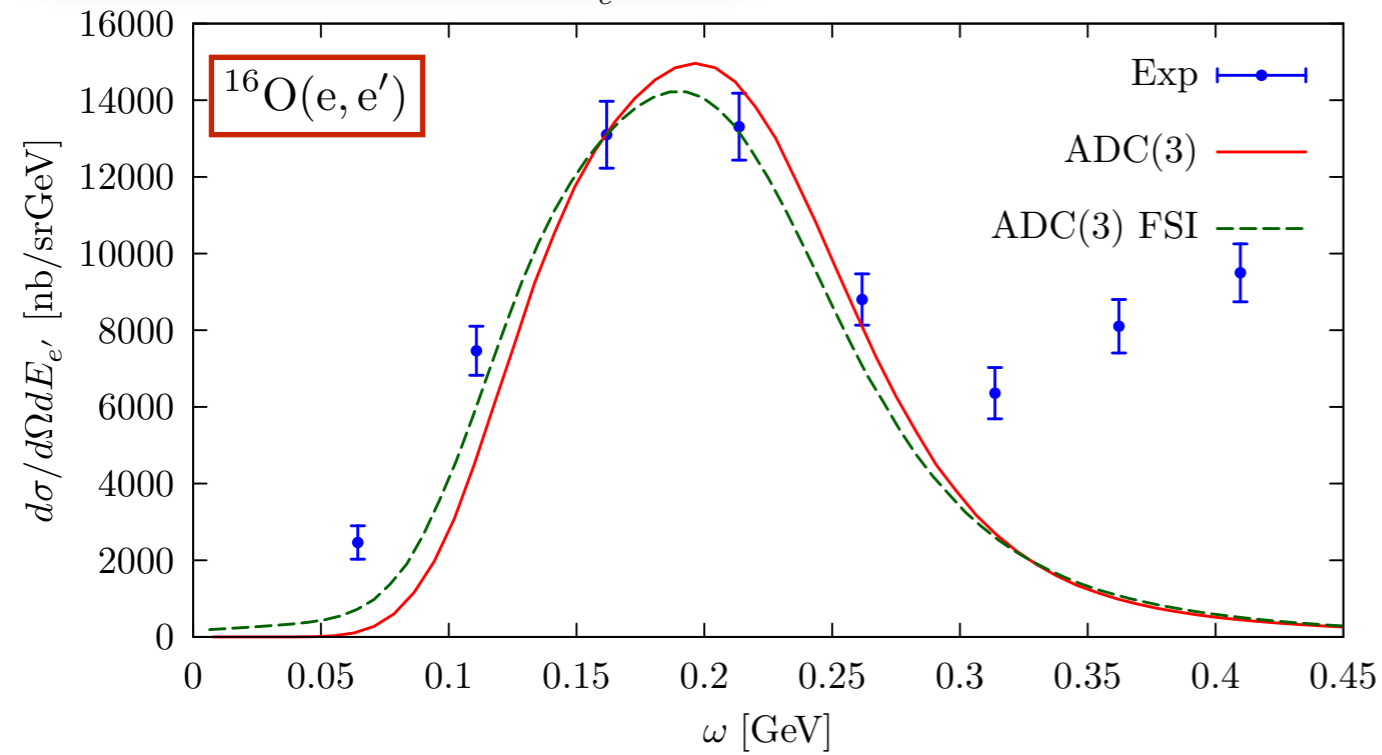
V. Somà, C. Barbieri, NR, in preparation

- The neutron structure of ^{40}Ar corresponds to the proton Ti isotopic chain

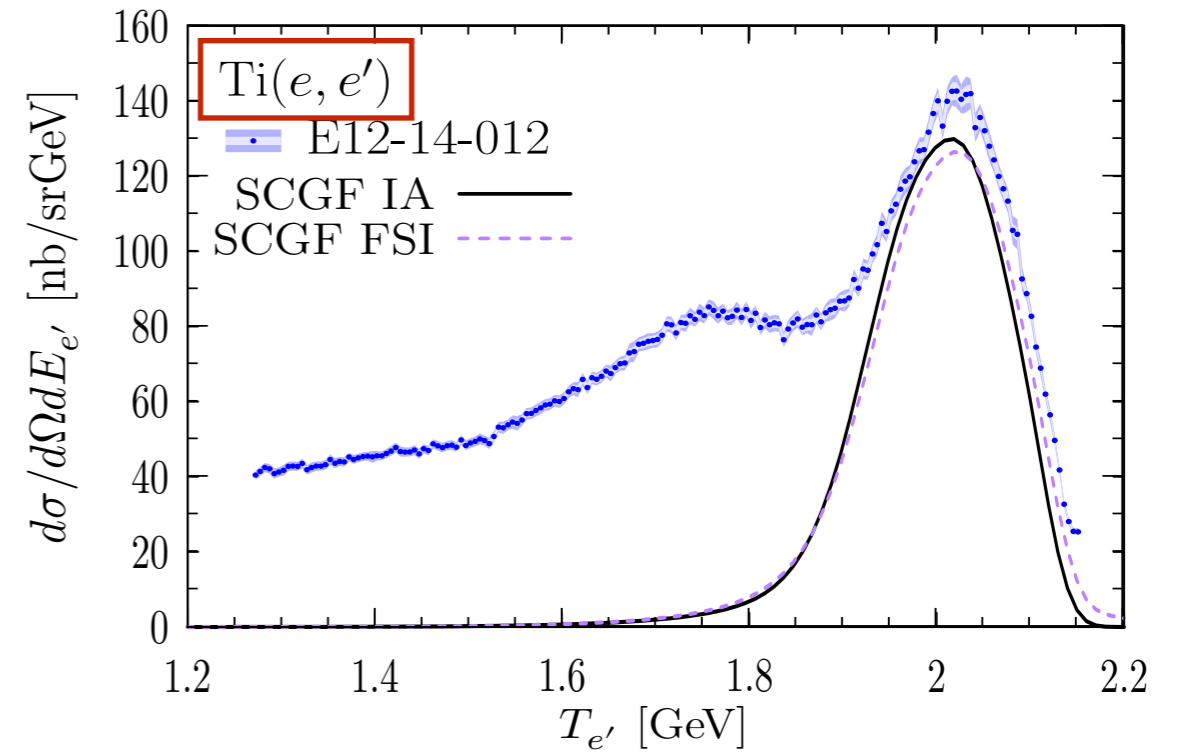
Electroweak scattering cross sections: 1b

NR, C. Barbieri, PRC98 (2018) 025501

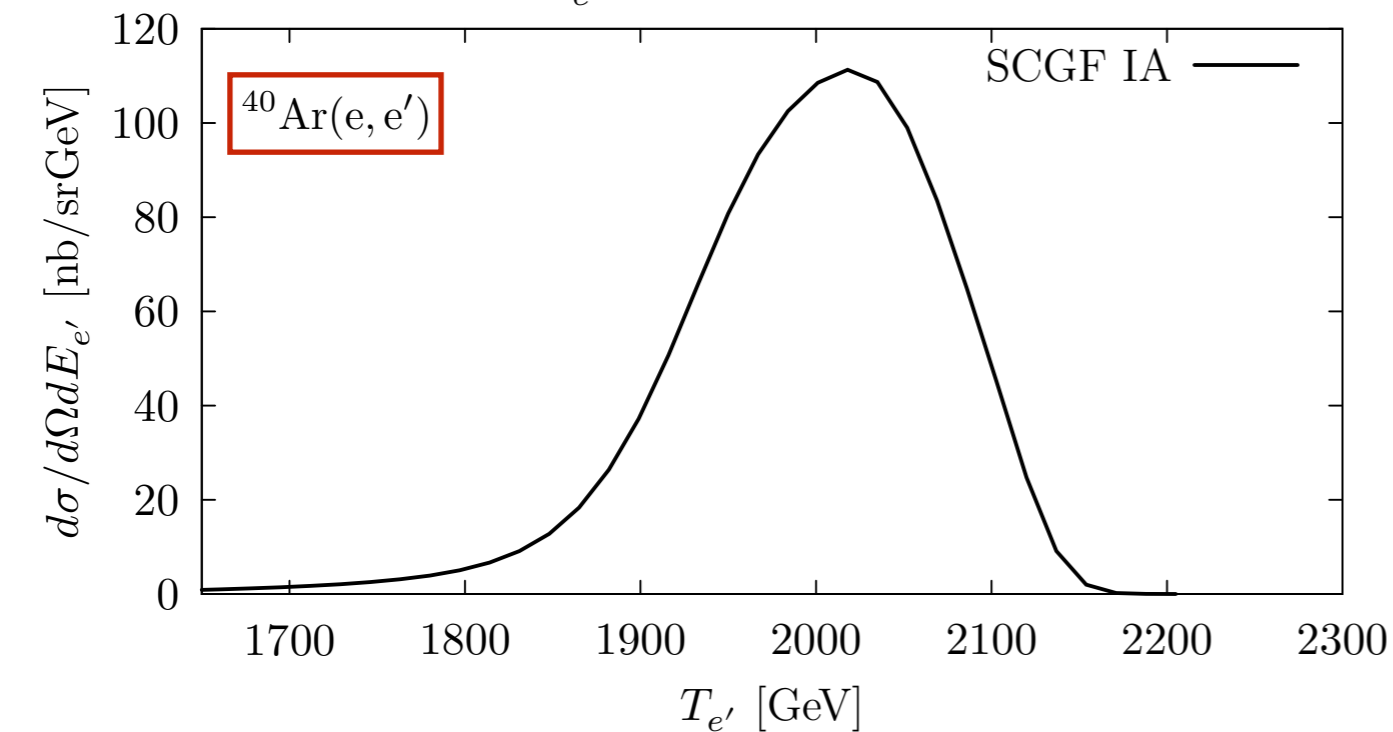
$E_e = 1080$ MeV $\theta = 32^\circ$



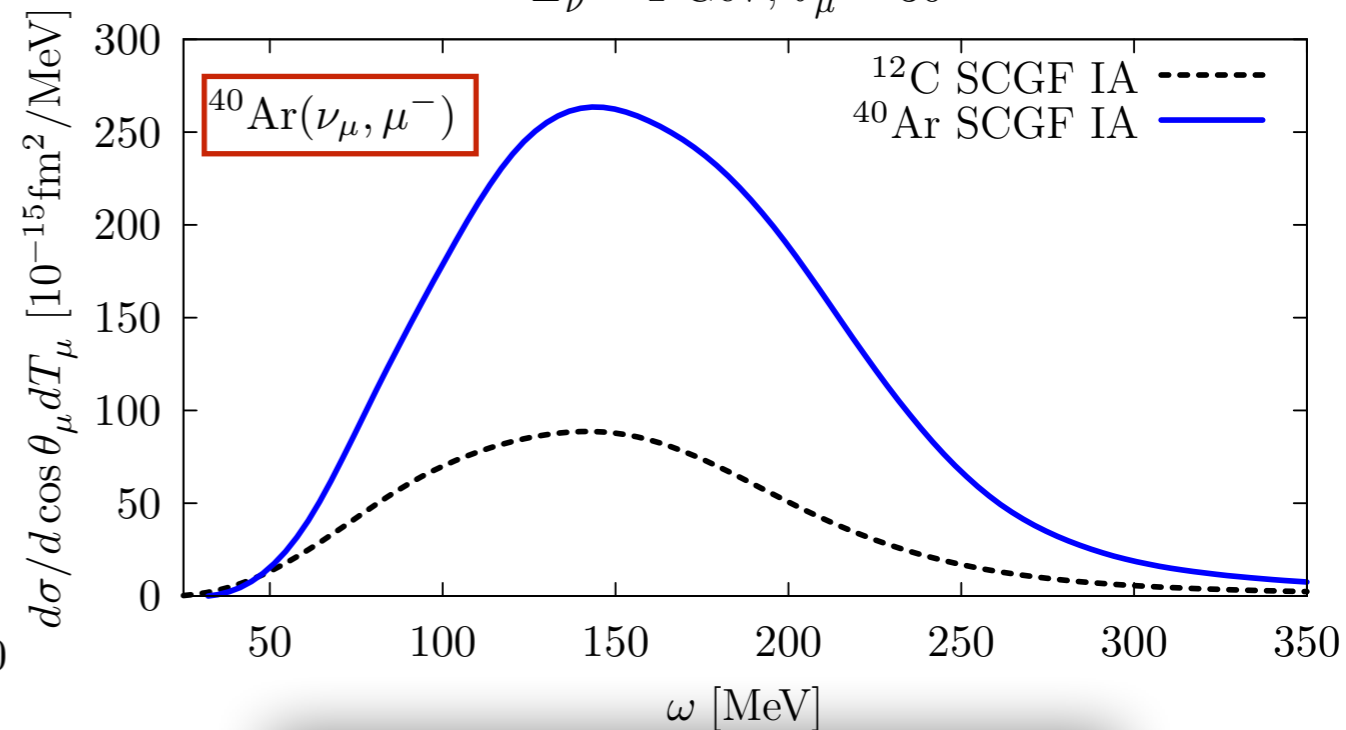
$E_e = 2.2$ GeV $\theta = 15.5^\circ$



$E_e = 2.2$ GeV $\theta = 15.5^\circ$



$E_\nu = 1$ GeV, $\theta_\mu = 30^\circ$



V. Somà, C. Barbieri, NR in Preparation

The CBF one-body Spectral Function of finite nuclei

- ^{12}C Spectral Function obtained within CBF and using the Local Density Approximation

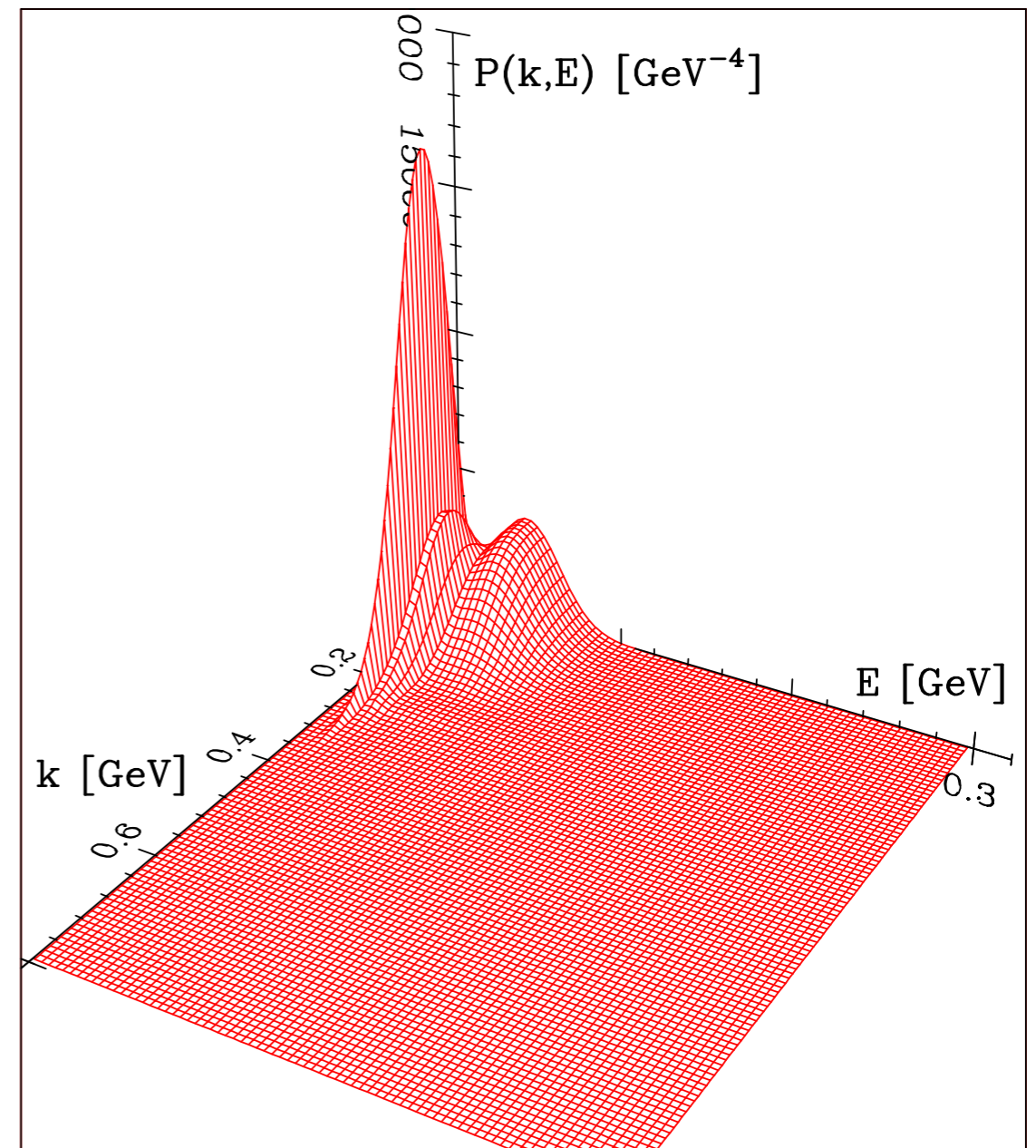
$$P_{LDA}(\mathbf{k}, E) = P_{MF}(\mathbf{k}, E) + P_{corr}(\mathbf{k}, E) \rightarrow \int d^3r P_{corr}^{NM}(\mathbf{k}, E; \rho = \rho_A(r))$$

$$\sum_n Z_n |\phi_n(\mathbf{k})|^2 F_n(E - E_n)$$

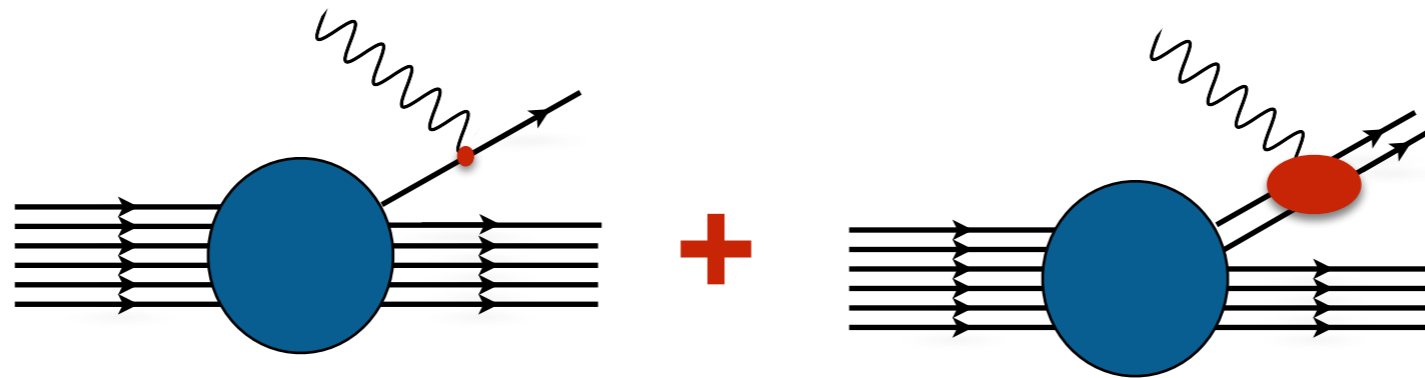
- Z_n : spectroscopic factor extracted from (e, e'p)
- F_n : finite width function accounting for residual interactions not included in a MF picture
- The one-body Spectral function of nuclear matter:

$$H = \sum_i \frac{\mathbf{p}_i^2}{2m} + \sum_{i < j} v_{ij} + \sum_{i < j < k} V_{ijk}$$

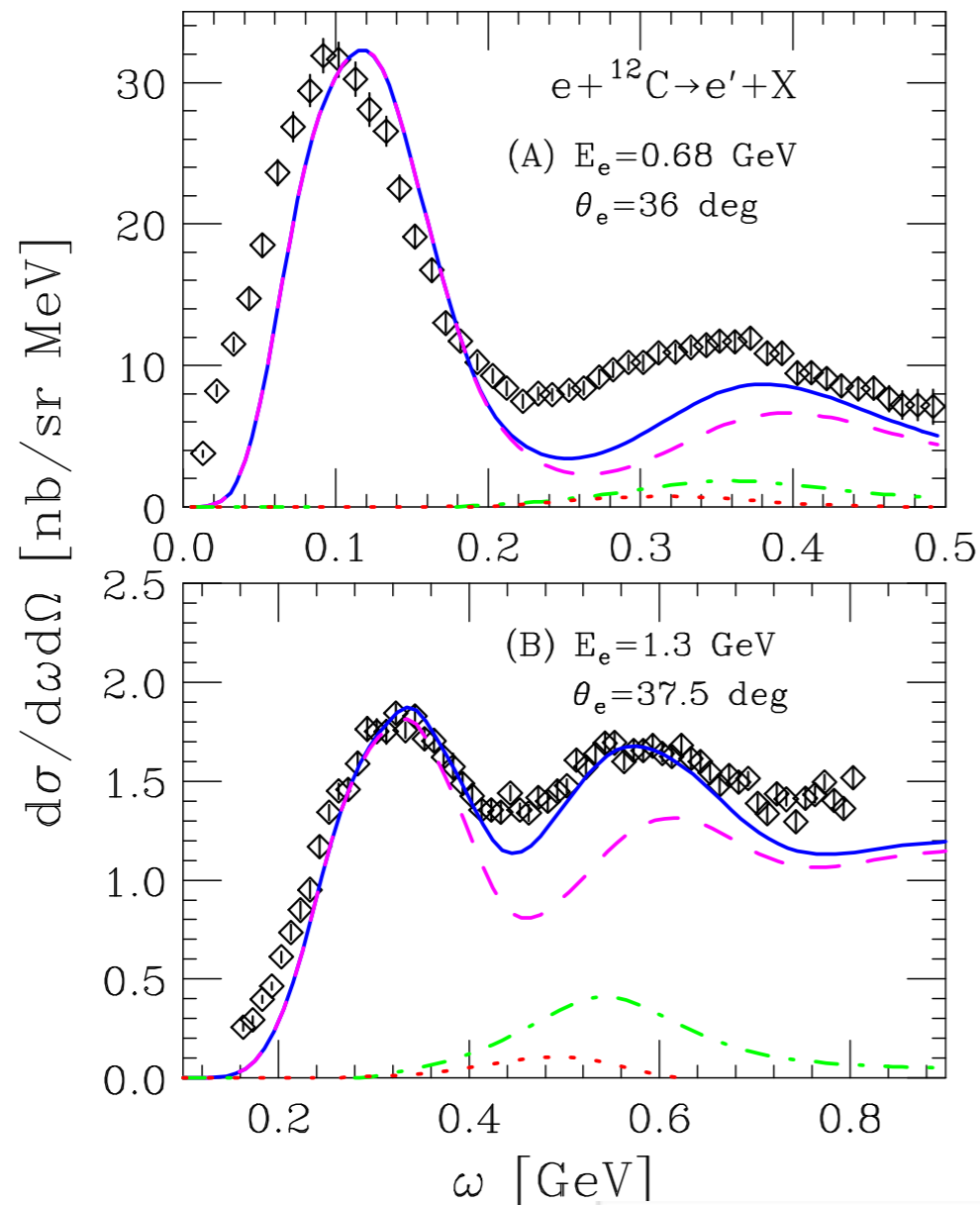
Argonne v18
UIX, IL7



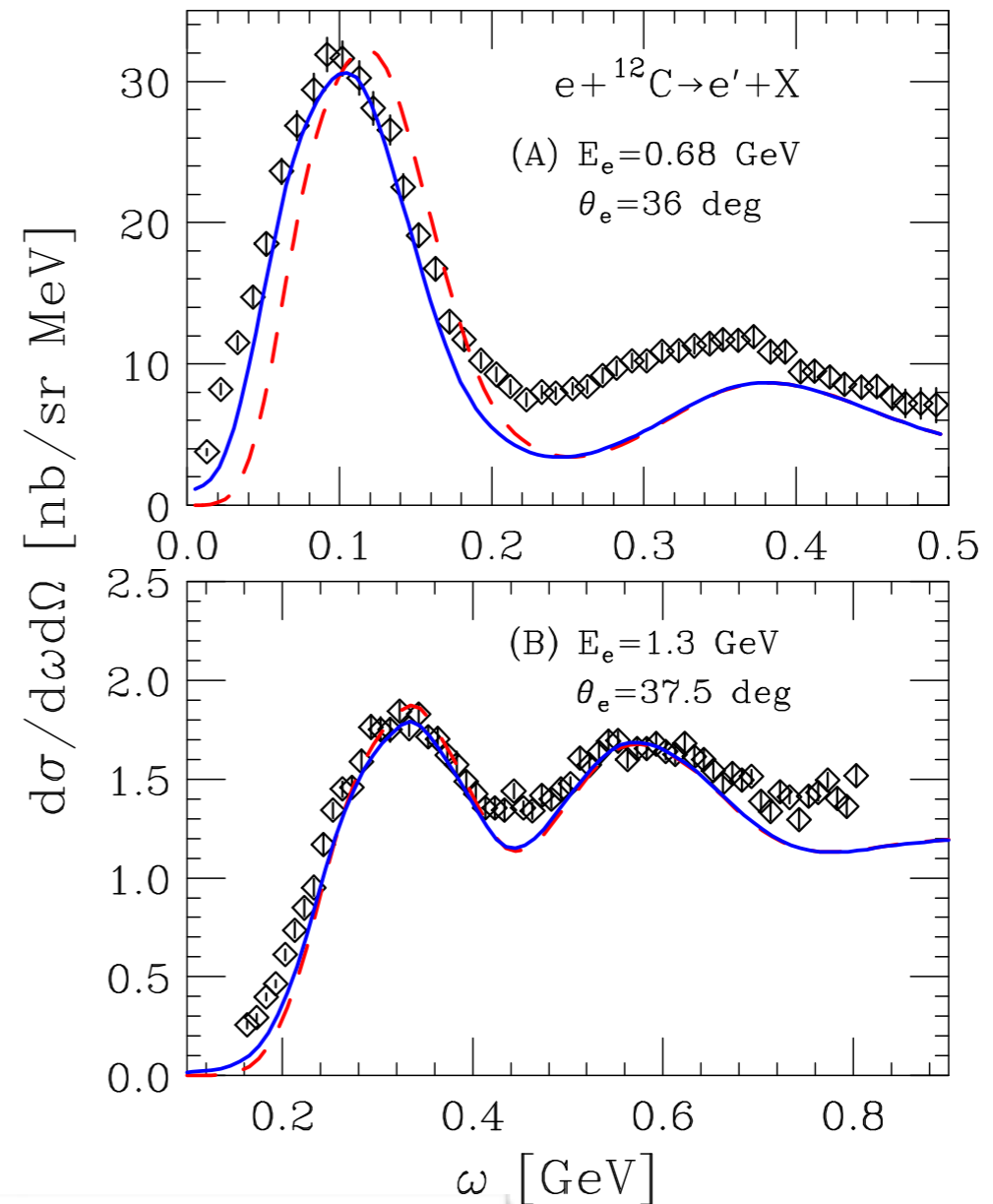
Results for $^{12}\text{C}(e,e')$ cross sections



- Separate contributions: IA



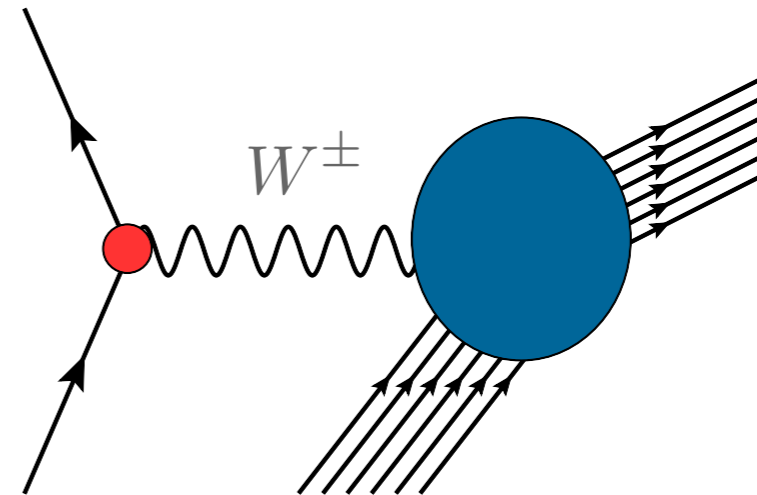
- Including FSI in the QE region



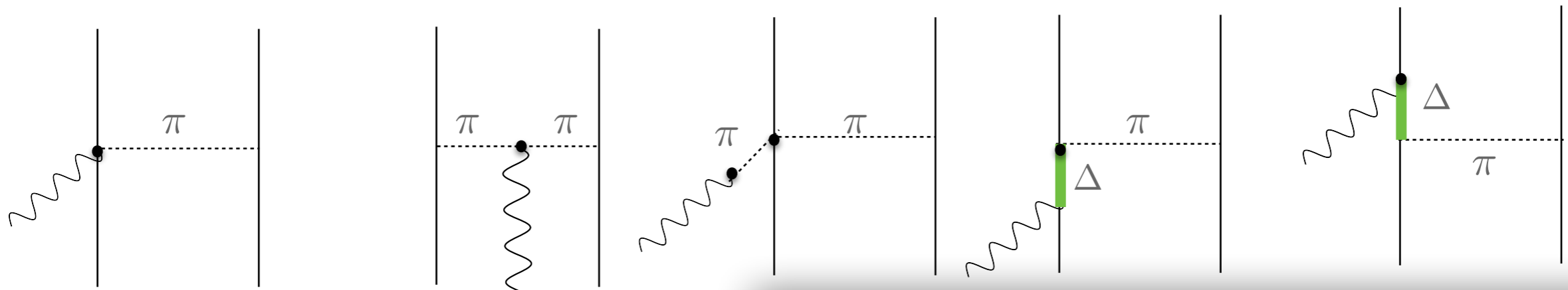
(Anti)neutrino -¹²C scattering cross sections

The inclusive cross section of the process in which a neutrino or antineutrino scatters off a nucleus can be written in terms of five response functions

$$\frac{d\sigma}{dE_{\ell'} d\Omega_{\ell'}} \propto [v_{00}R_{00} + v_{zz}R_{zz} - v_{0z}R_{0z} + v_{xx}R_{xx} \mp v_{xy}R_{xy}]$$



- We generalized the SF formalism to include vector and axial vector relativistic two-body currents

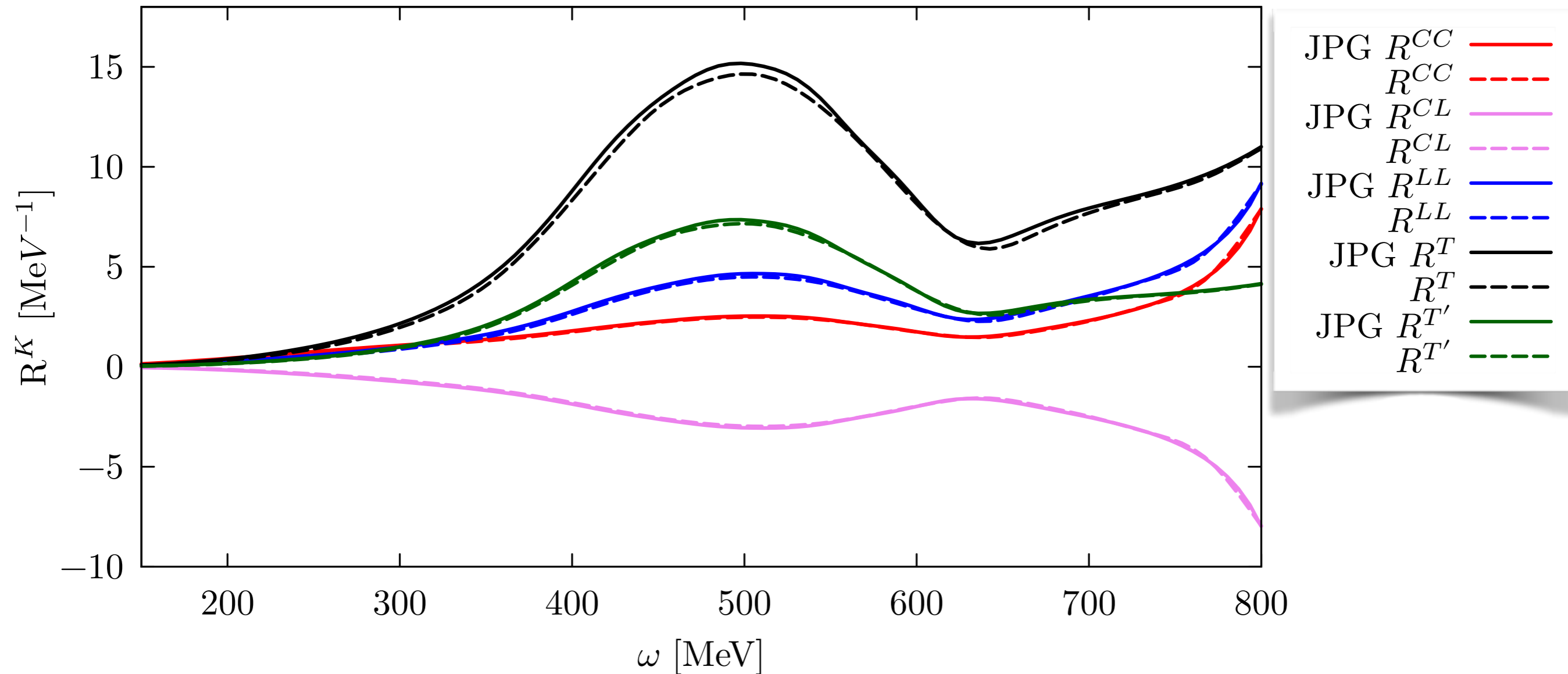


NR, C.Barbieri, O. Benhar, A. De Pace, A. Lovato, in Preparation

- The calculation of the MEC current matrix is carried out automatically
- 9d-integral + use of realistic SFs implies dealing with a broader phase space: we developed an highly parallel Monte Carlo code, importance sampling procedure

Two-body CC response functions of ^{12}C

$q=800$ MeV



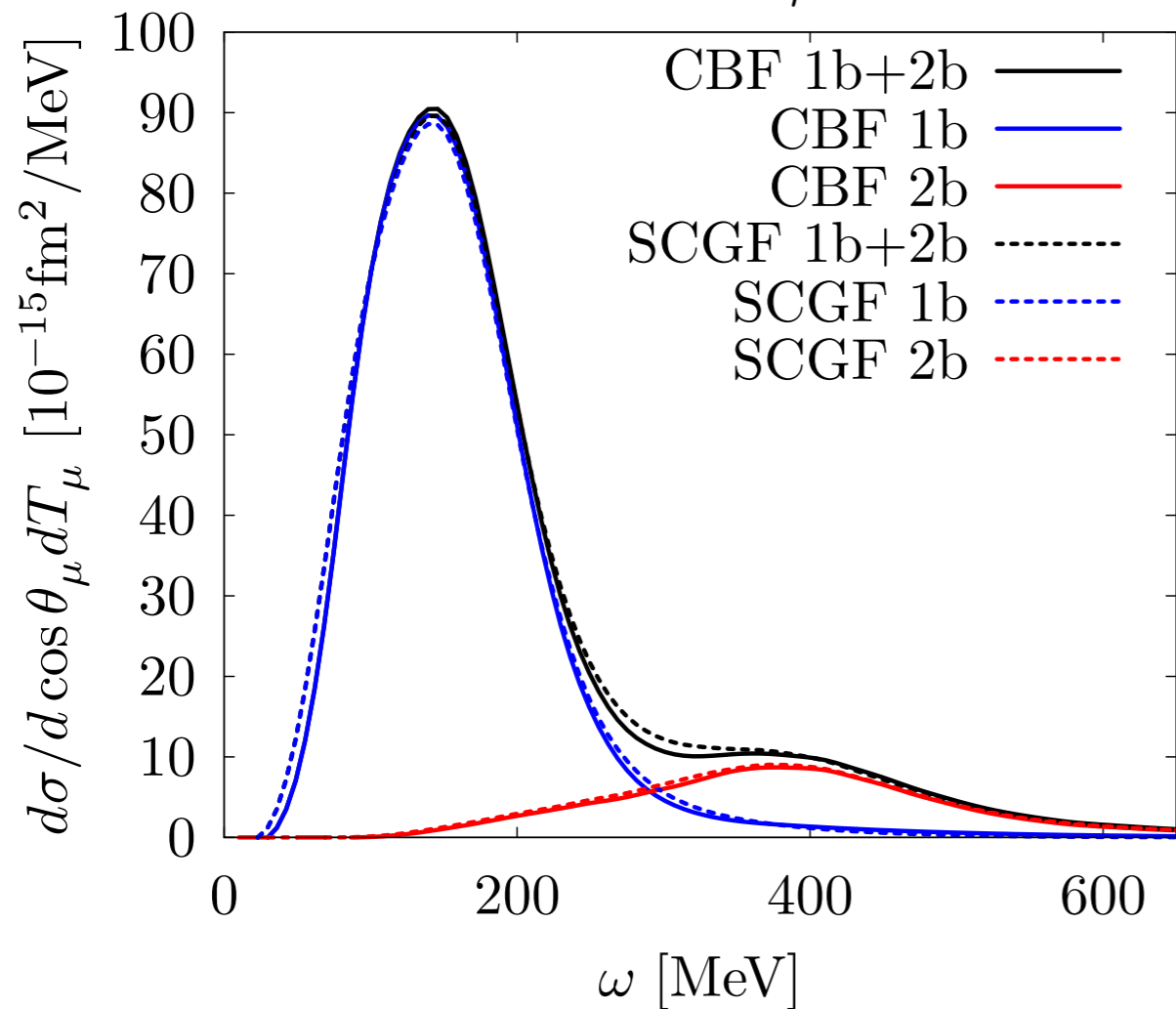
• Comparison of the five CC response functions of ^{12}C with the results of [I. Ruiz Simo, et. al, Journal of Phys. G 44, no. 6 \(2017\)](#).

• In this case, we approximated the two-body spectral function with that of the global relativistic Fermi gas model

CCQE neutrino -¹²C cross sections

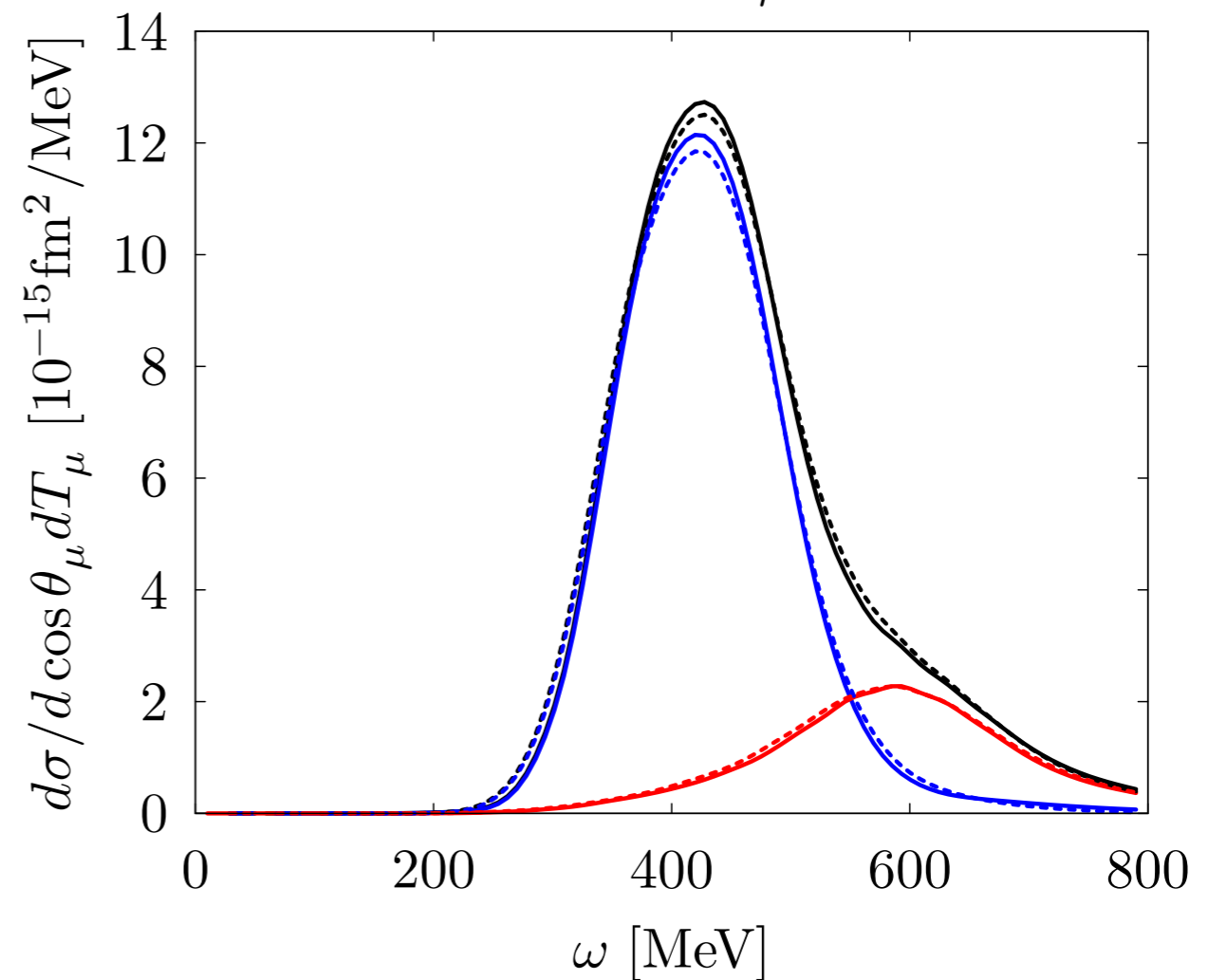
$$\nu_{\mu} + {}^{12}\text{C} \rightarrow \mu^{-} + X$$

$$E_{\nu} = 1 \text{ GeV}, \theta_{\mu} = 30^{\circ}$$

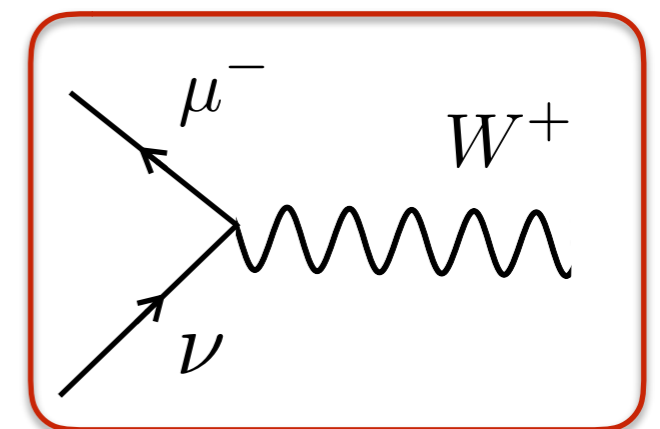


NR, C.Barbieri, O. Benhar, A. De Pace, A. Lovato, in Preparation

$$E_{\nu} = 1 \text{ GeV}, \theta_{\mu} = 70^{\circ}$$



- The 2b contribution mostly affects the ‘dip’ region, in analogy with the electromagnetic case
- Meson exchange currents strongly enhance the cross section for large values of the scattering angle

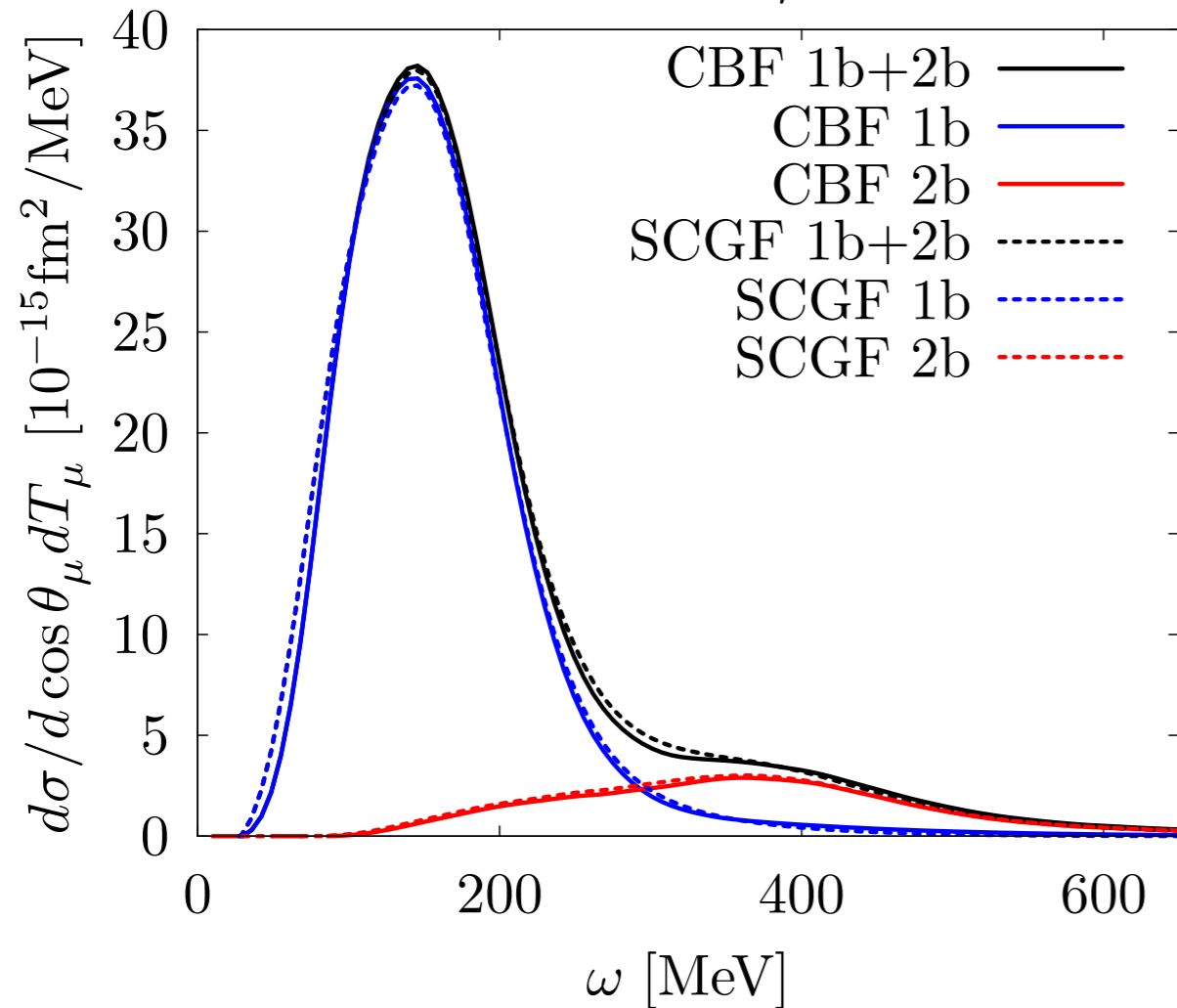


CCQE antineutrino -¹²C cross sections

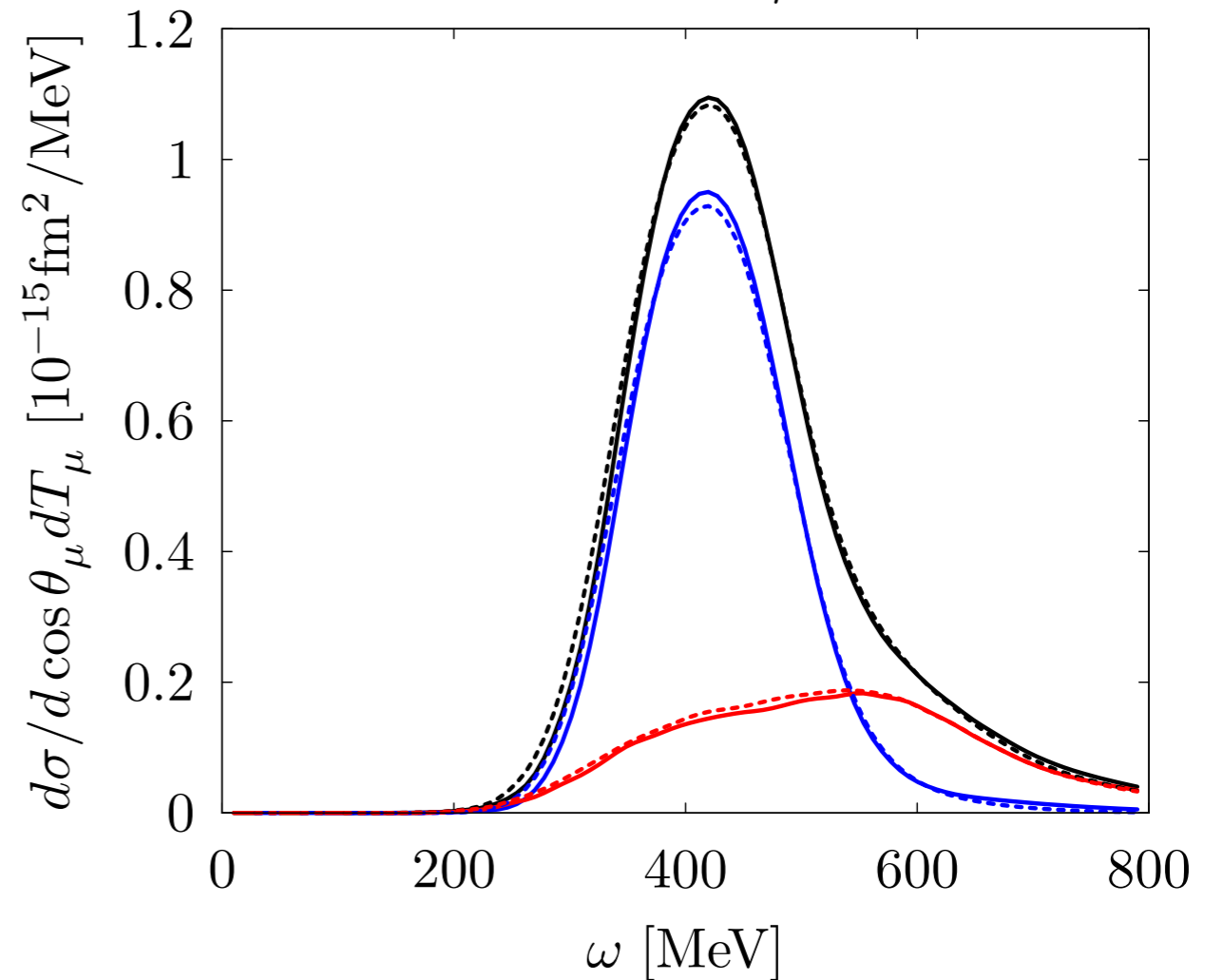
$$\bar{\nu}_\mu + {}^{12}\text{C} \rightarrow \mu^+ + \text{X}$$

NR, C.Barbieri, O. Benhar, A. De Pace, A. Lovato, in Preparation

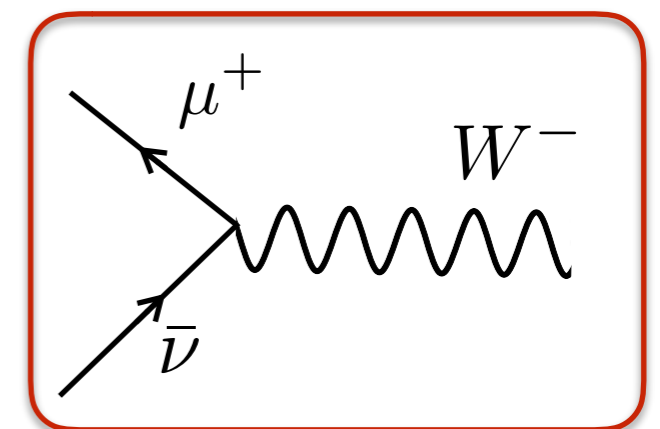
$$E_{\bar{\nu}} = 1 \text{ GeV}, \theta_\mu = 30^\circ$$



$$E_{\bar{\nu}} = 1 \text{ GeV}, \theta_\mu = 70^\circ$$



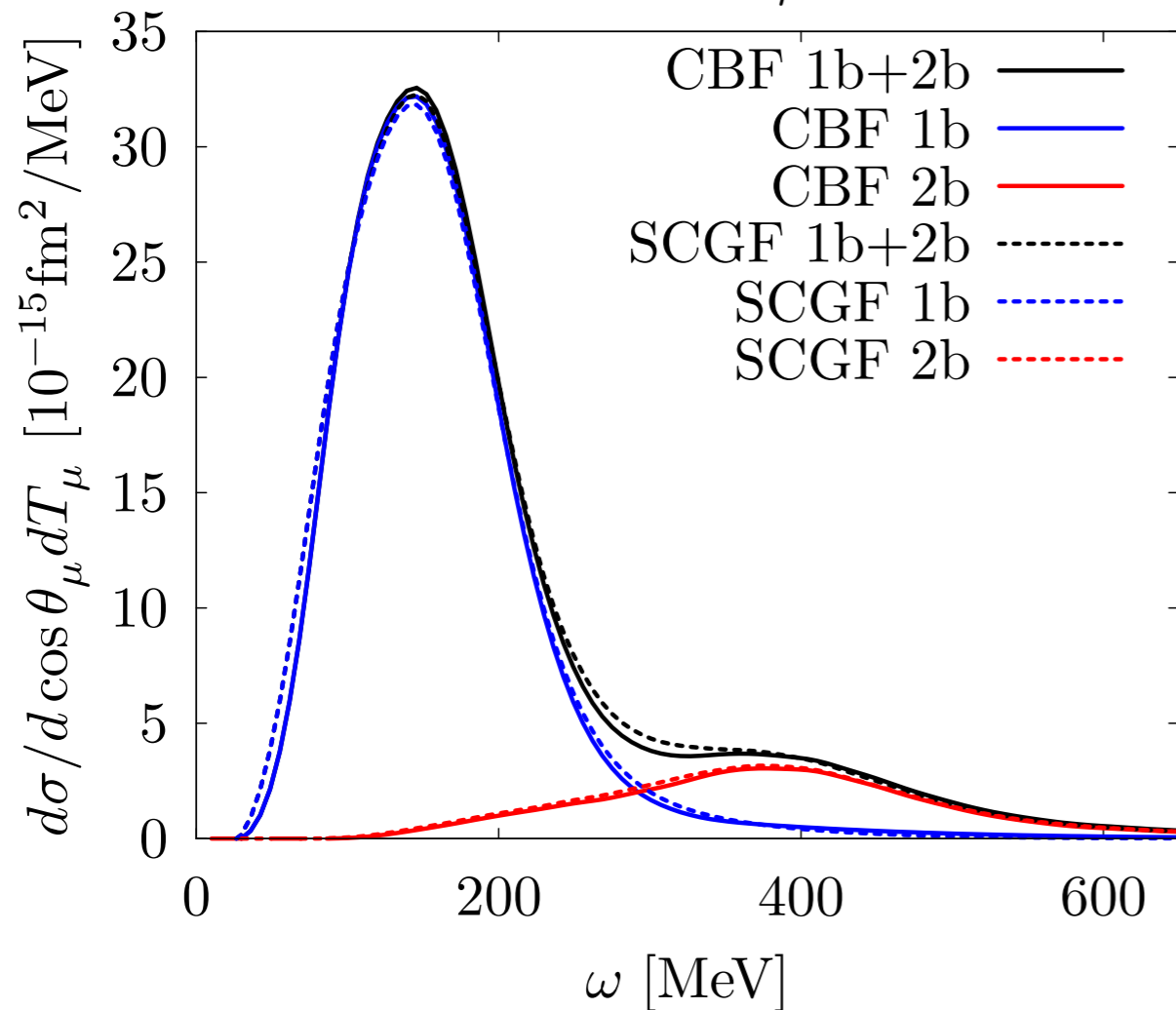
- The 2b contribution mostly affects the ‘dip’ region, in analogy with the electromagnetic case
- Meson exchange currents strongly enhance the cross section for large values of the scattering angle



NCQE neutrino -¹²C cross sections

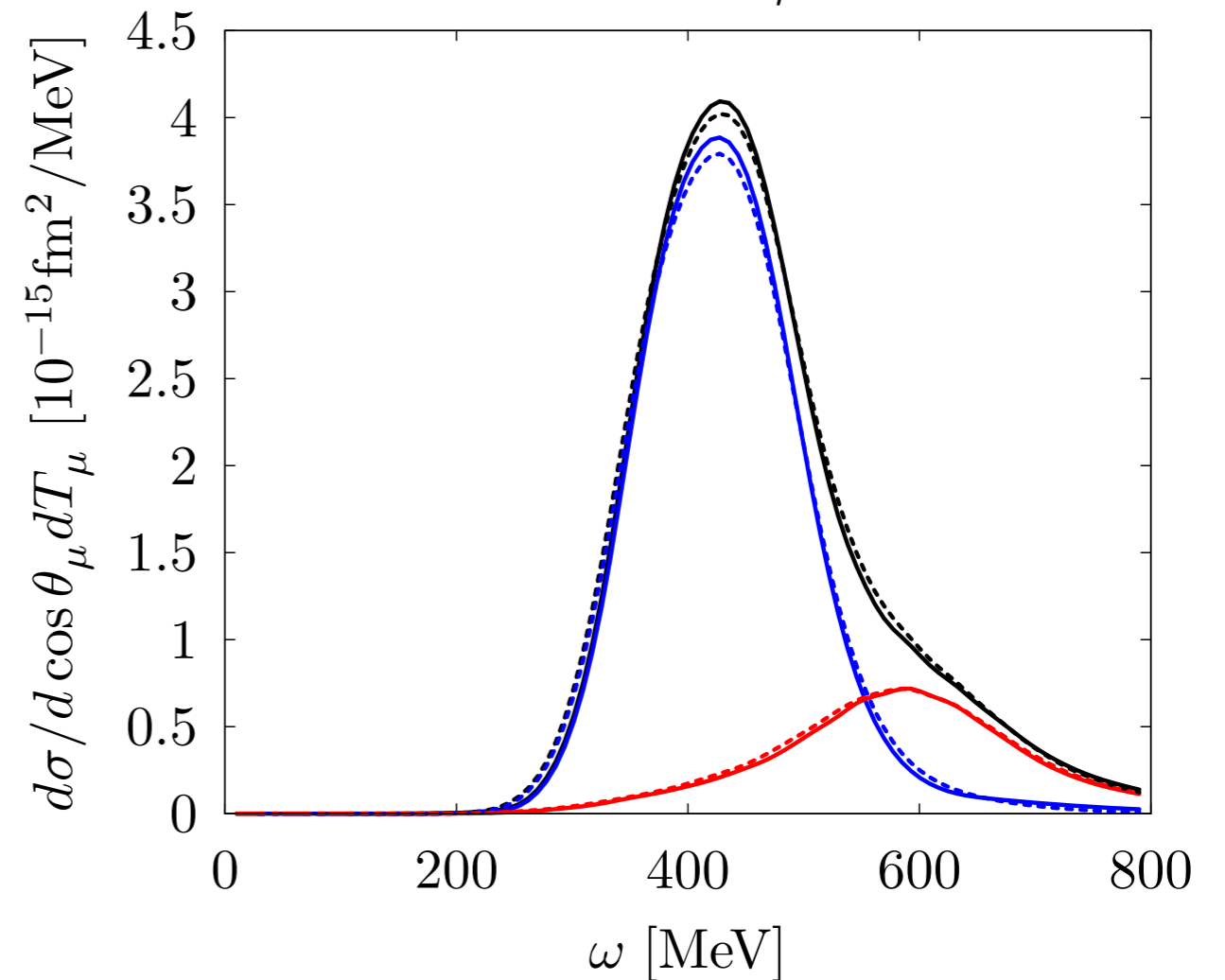
$$\nu_\mu + {}^{12}\text{C} \rightarrow \nu_\mu + X$$

$$E_\nu = 1 \text{ GeV}, \theta_\mu = 30^\circ$$

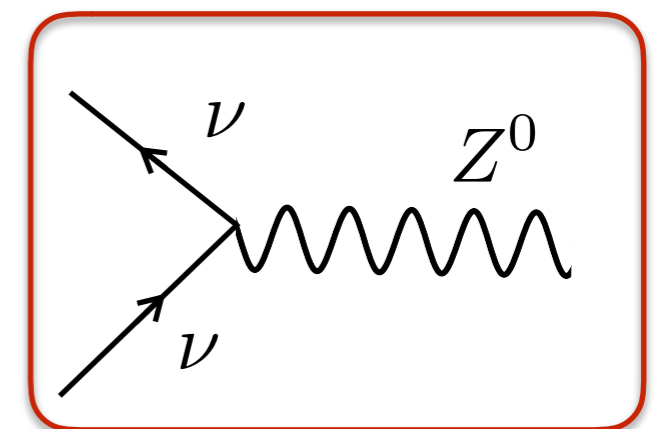


NR, C.Barbieri, O. Benhar, A. De Pace, A. Lovato, in Preparation

$$E_\nu = 1 \text{ GeV}, \theta_\mu = 70^\circ$$



- The 2b contribution mostly affects the ‘dip’ region, in analogy with the electromagnetic case
- Meson exchange currents strongly enhance the cross section for large values of the scattering angle

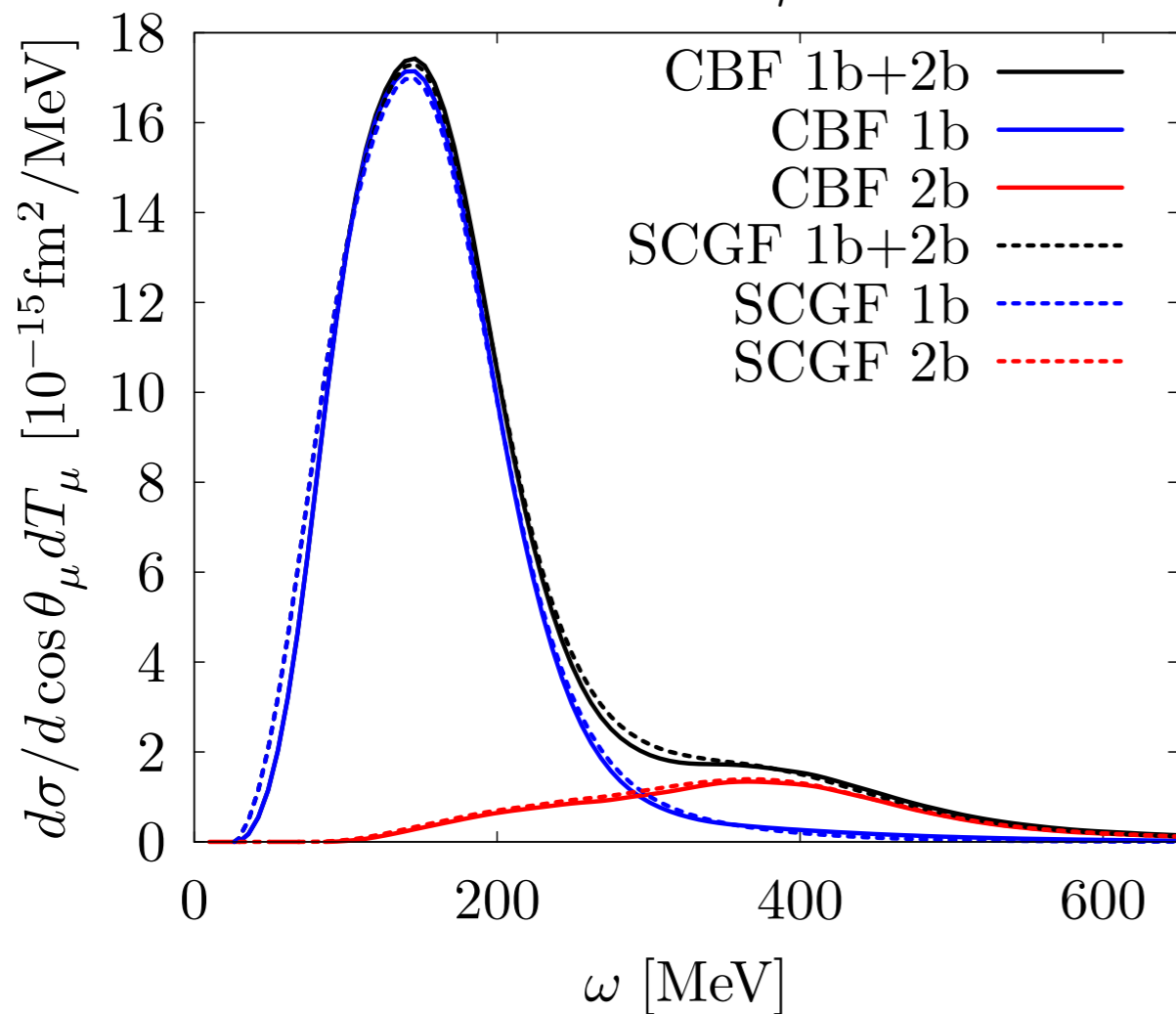


NCQE antineutrino -¹²C cross sections

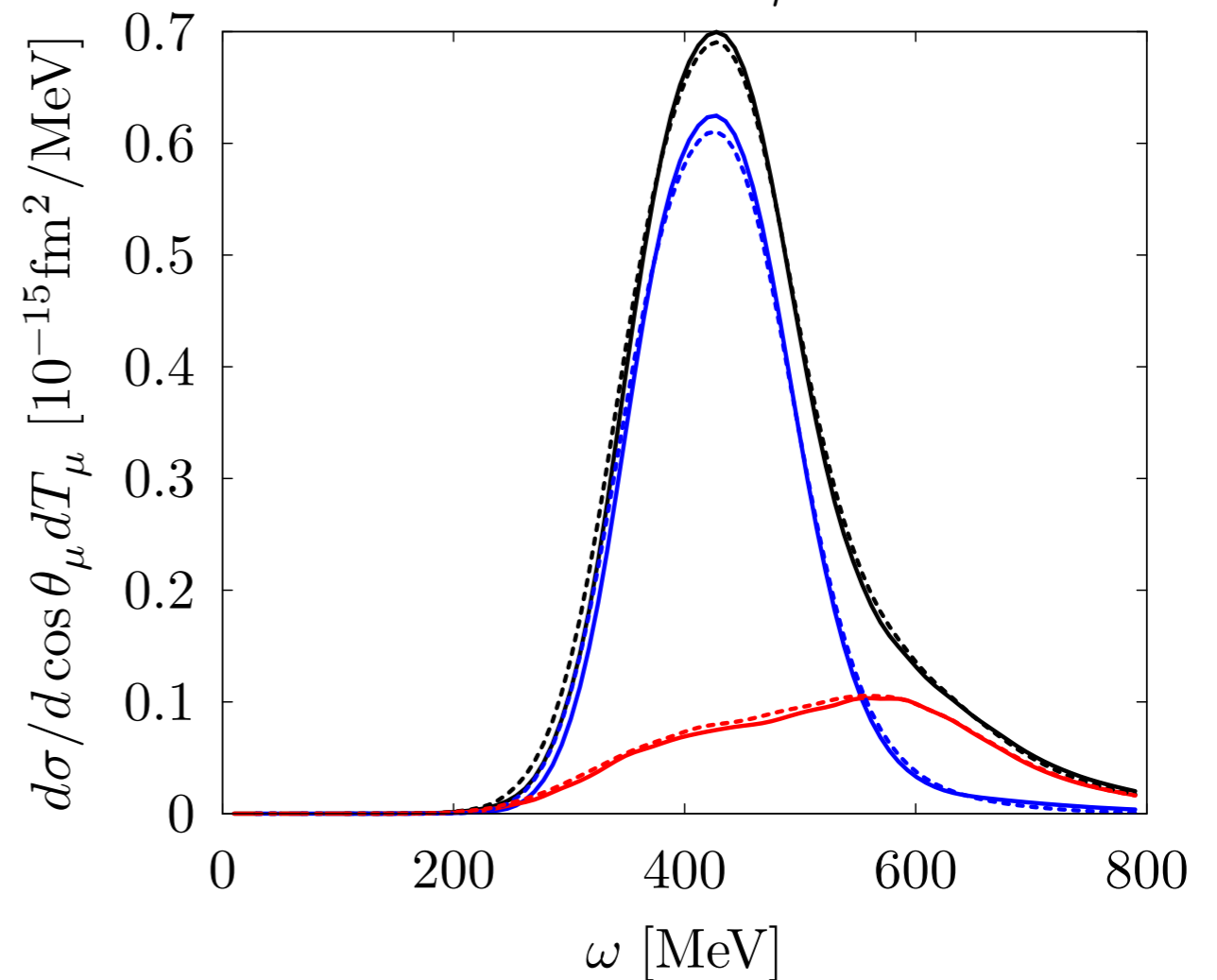
$$\bar{\nu}_\mu + {}^{12}\text{C} \rightarrow \bar{\nu}_\mu + X$$

NR, C.Barbieri, O. Benhar, A. De Pace, A. Lovato, in Preparation

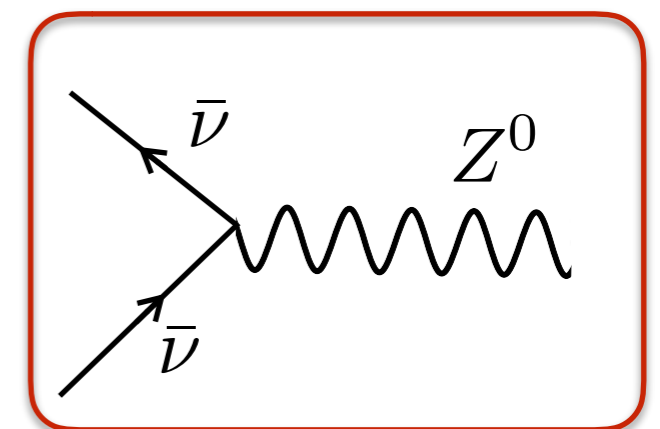
$$E_{\bar{\nu}} = 1 \text{ GeV}, \theta_\mu = 30^\circ$$



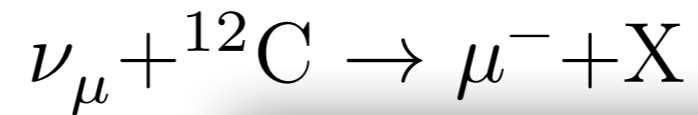
$$E_{\bar{\nu}} = 1 \text{ GeV}, \theta_\mu = 70^\circ$$



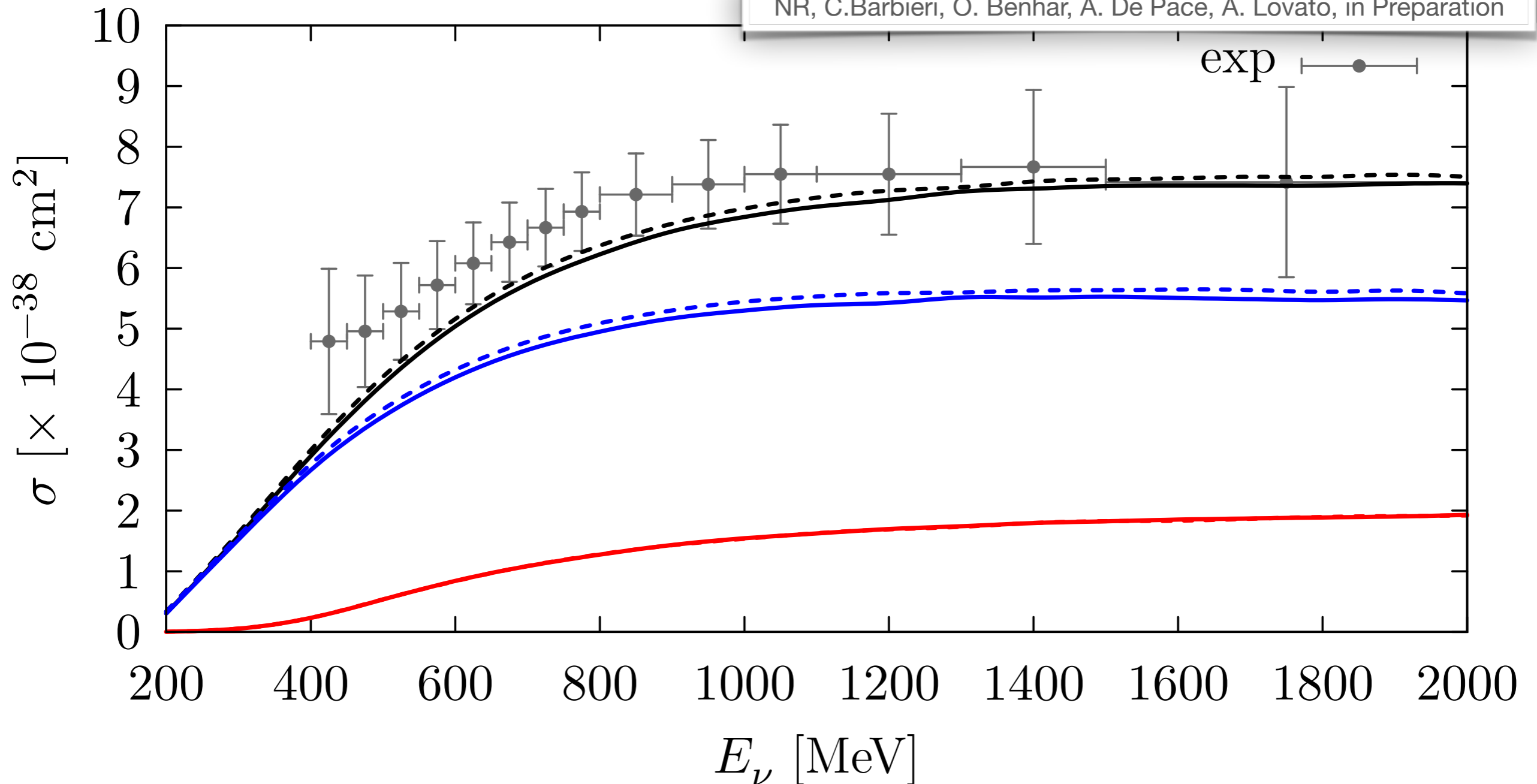
- The 2b contribution mostly affects the ‘dip’ region, in analogy with the electromagnetic case
- Meson exchange currents strongly enhance the cross section for large values of the scattering angle



CCQE neutrino -¹²C total cross section

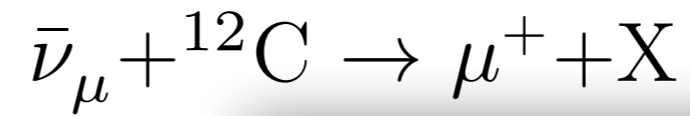


NR, C.Barbieri, O. Benhar, A. De Pace, A. Lovato, in Preparation

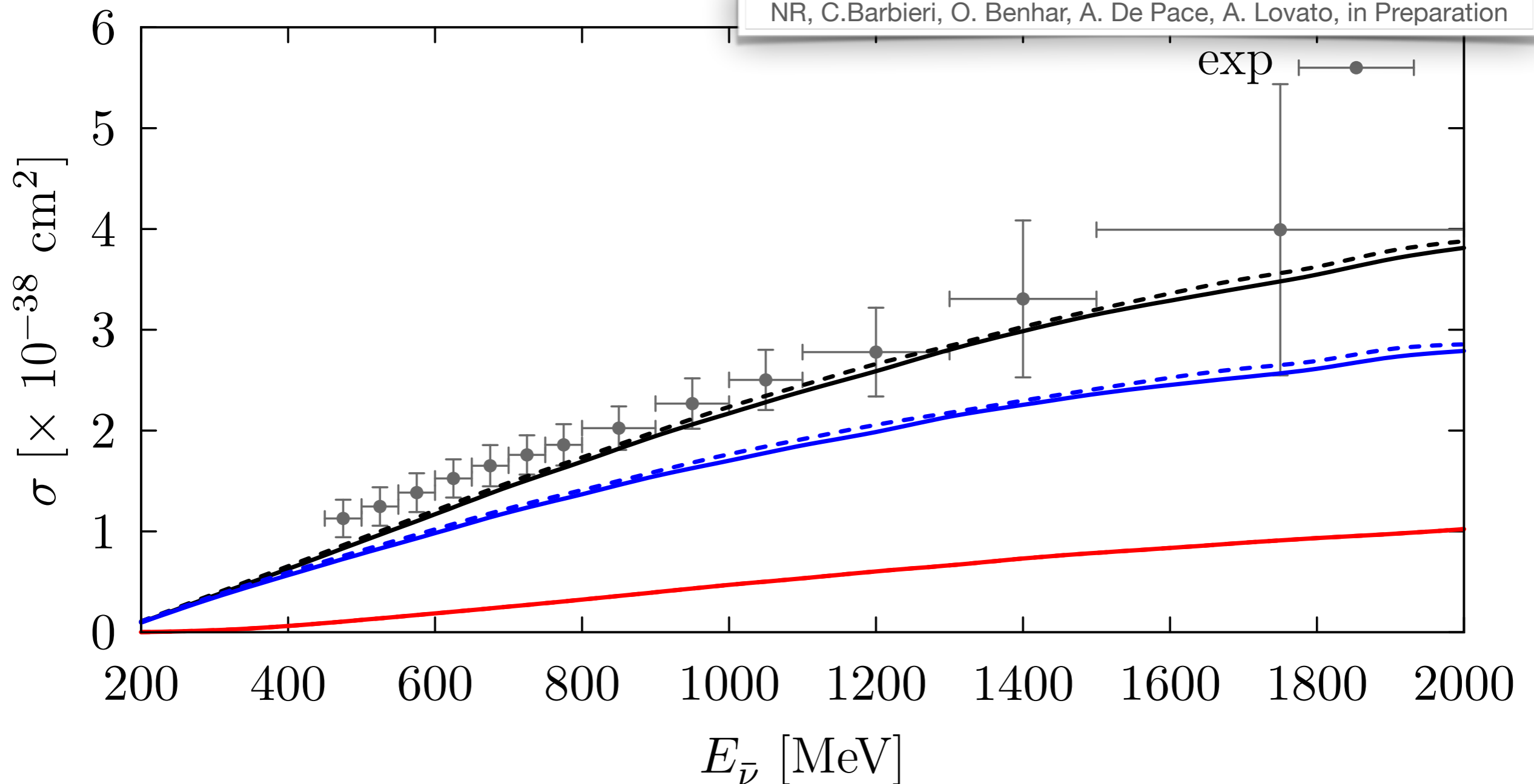


- The 2p2h contribution is needed to explain the size of the measured cross section

CCQE antineutrino -¹²C total cross section



NR, C.Barbieri, O. Benhar, A. De Pace, A. Lovato, in Preparation



- The 2p2h contribution is needed to explain the size of the measured cross section

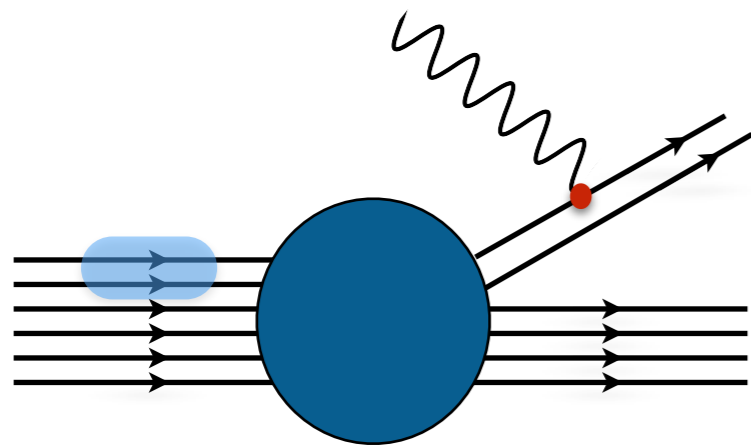
Prospects

- Correlated Basis Function and Self Consistent Green's Function approach :
 - ❖ Flux-folded double differential inclusive cross sections for CC and NCQE processes
 - ❖ Inclusion of the interference between one- and two-body currents: benchmark with GFMC
 - ❖ Describe the resonance production region for CC and NC processes
 - ❖ Including the contribution of two-body currents in the ^{40}Ar and ^{48}Ti scattering cross sections results
- Green's Function Monte Carlo approach :
 - ❖ Inverting the Euclidean responses for CC processes
 - ❖ Spectral Function calculation of light nuclei within GFMC with both phenomenological and chiral Hamiltonians
 - ❖ The use of different potentials can provide an estimate of the theoretical uncertainty of the calculation

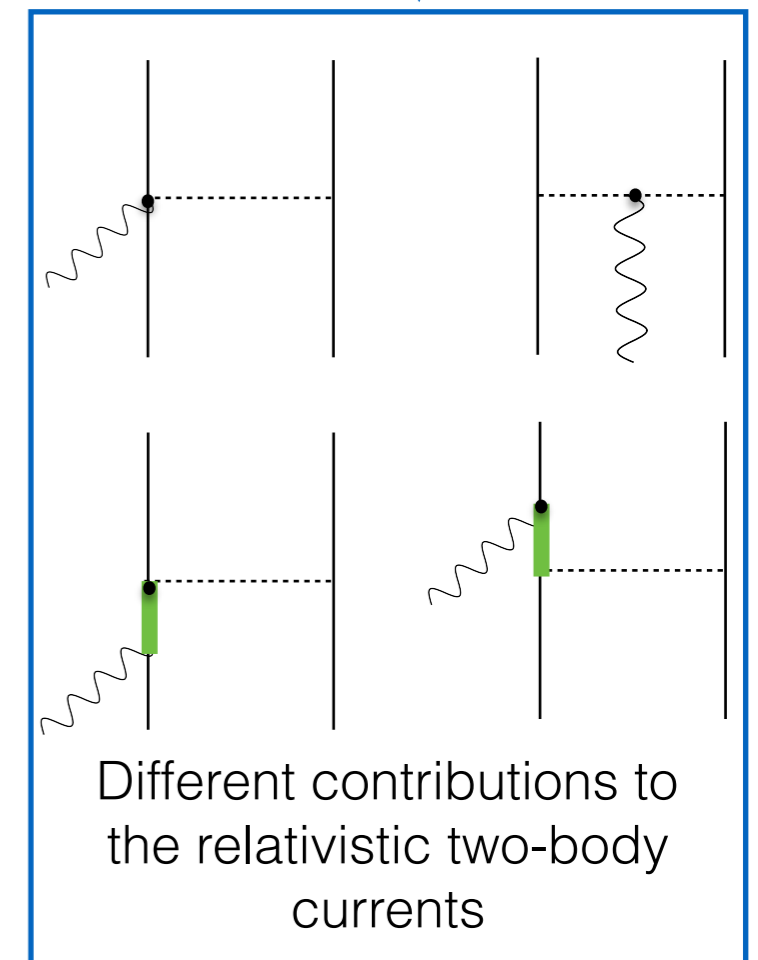
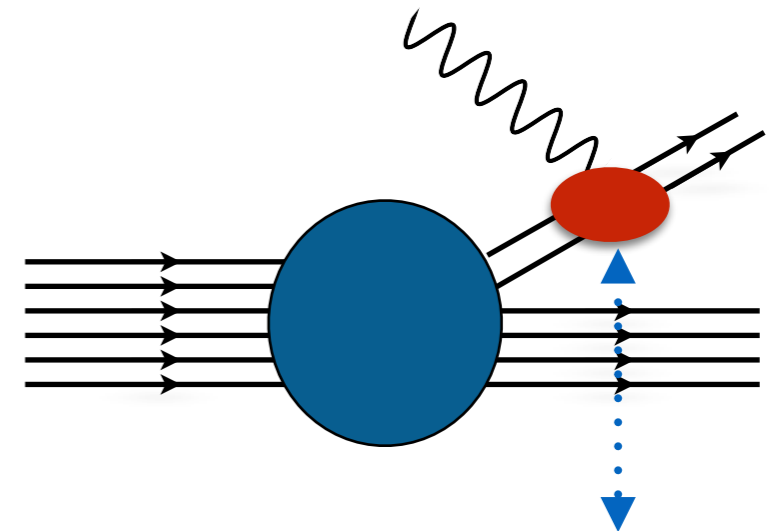
Back up slides

Production of two particle-two hole (2p2h) states

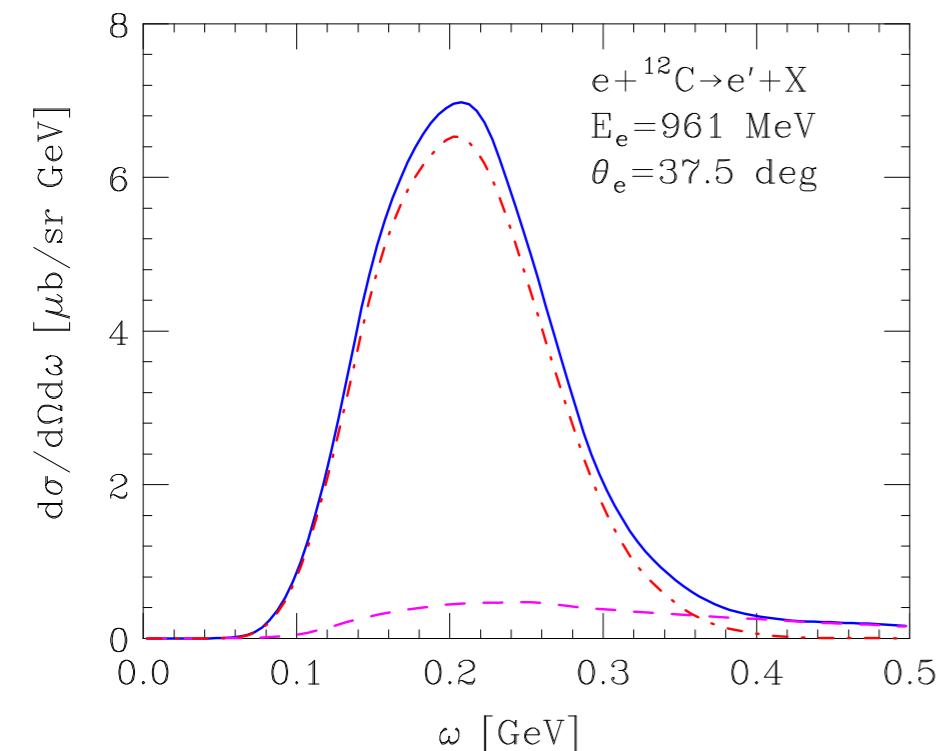
- Initial State Correlations



- Meson Exchange currents



- $P_{\text{corr}}(\mathbf{k}, E)$ accounts for the presence of strongly correlated pairs. Its contribution to the cross section is clearly visible: appearance of a tail in the large energy transfer region



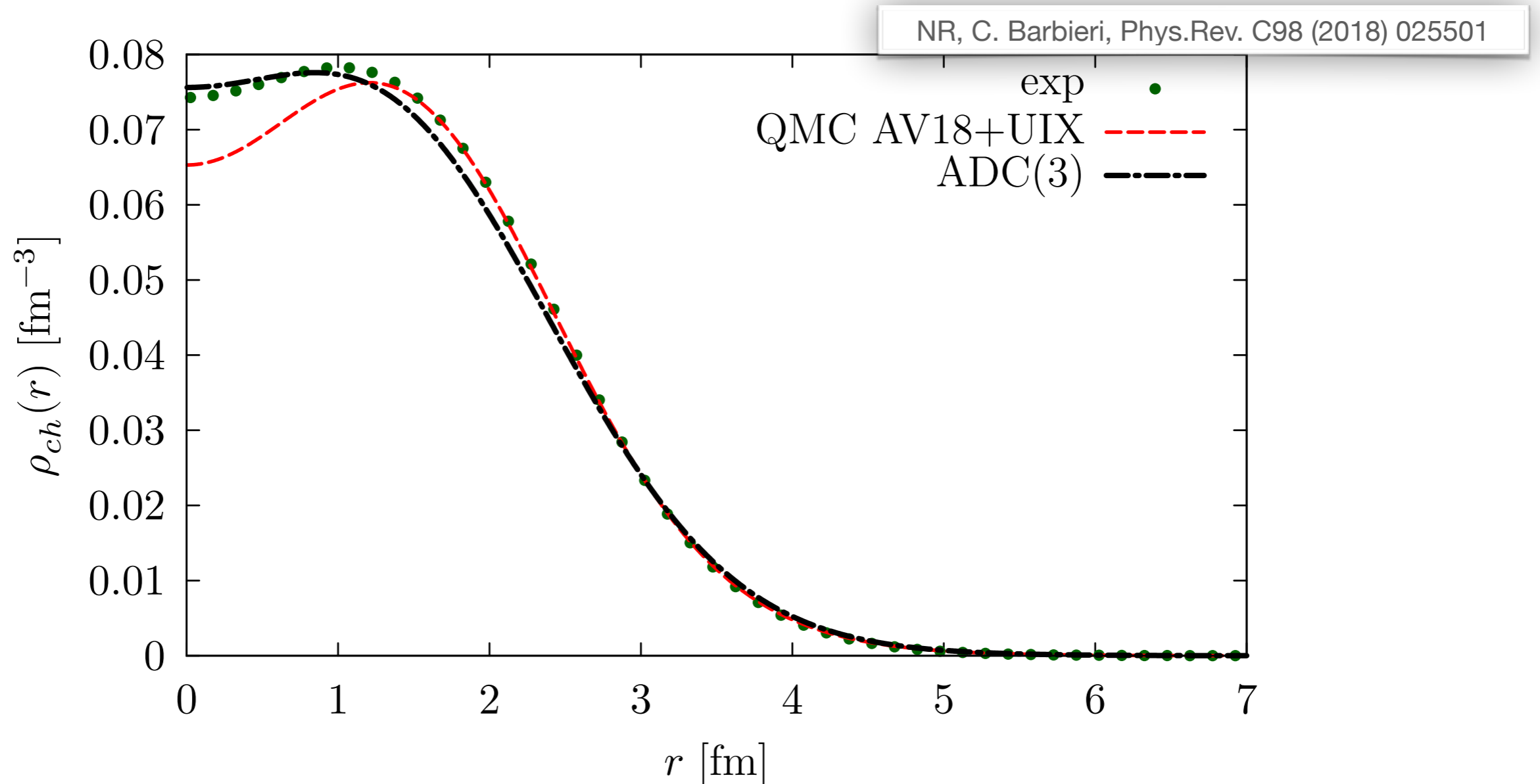
- The Impulse Approximation has been generalized:

$$W_{2p2h}^{\mu\nu} = W_{ISC}^{\mu\nu} + W_{MEC}^{\mu\nu} + W_{int}^{\mu\nu}$$

Benchmark the nuclear model: ^{16}O charge density distribution

- The nuclear charge density distribution is the Fourier transform of the charge elastic form factor:

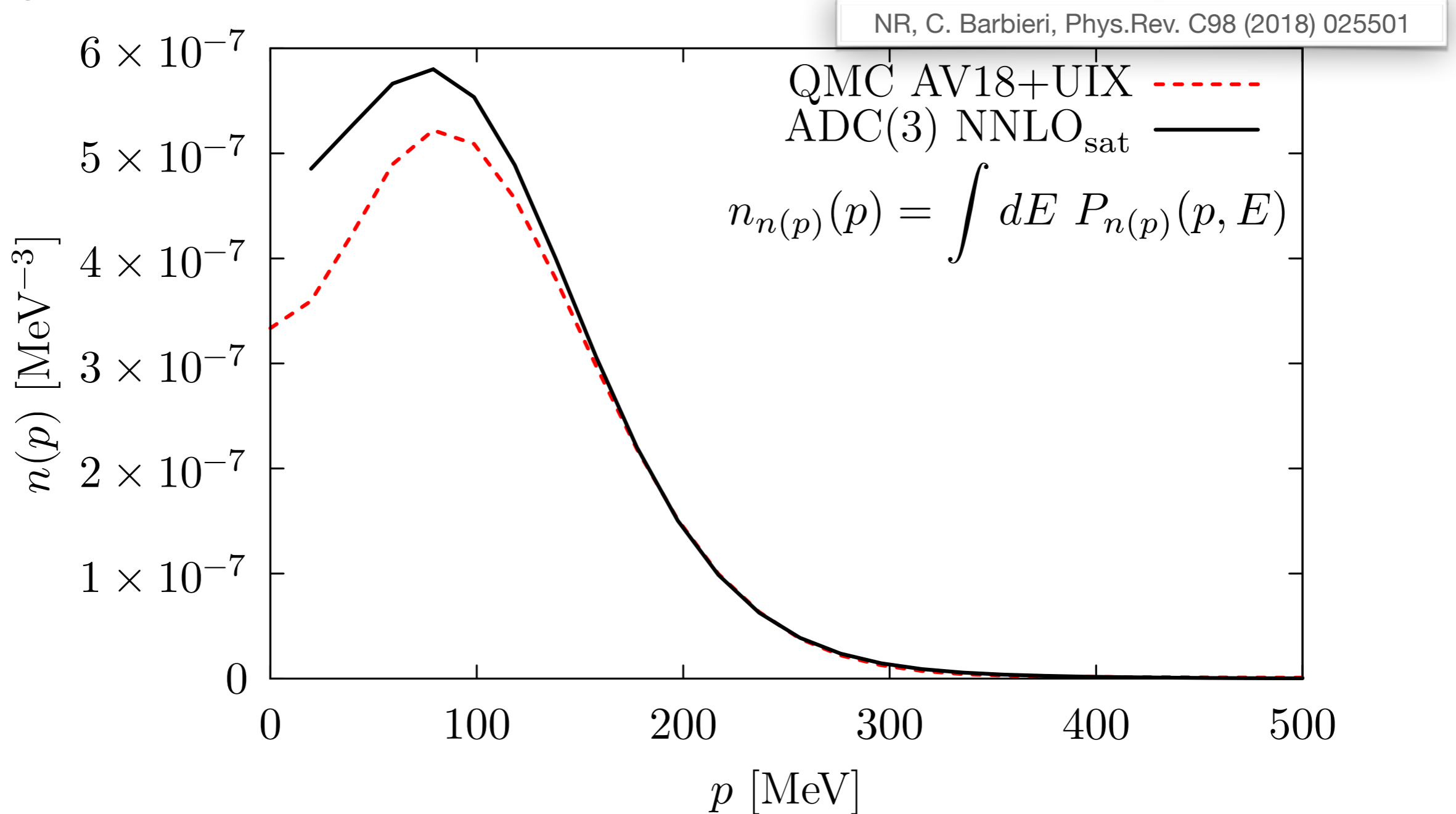
$$\rho_{ch}(r') = \int \frac{d^3q}{(2\pi)^3} e^{-i\mathbf{q}\cdot\mathbf{r}'} F_L(\mathbf{q})$$



- Nice agreement between the SCGF and QMC calculations
- SCGF results agree with experiments (corroborates the goodness of NNLO_{sat})

Benchmark the nuclear model: ^{16}O momentum distribution

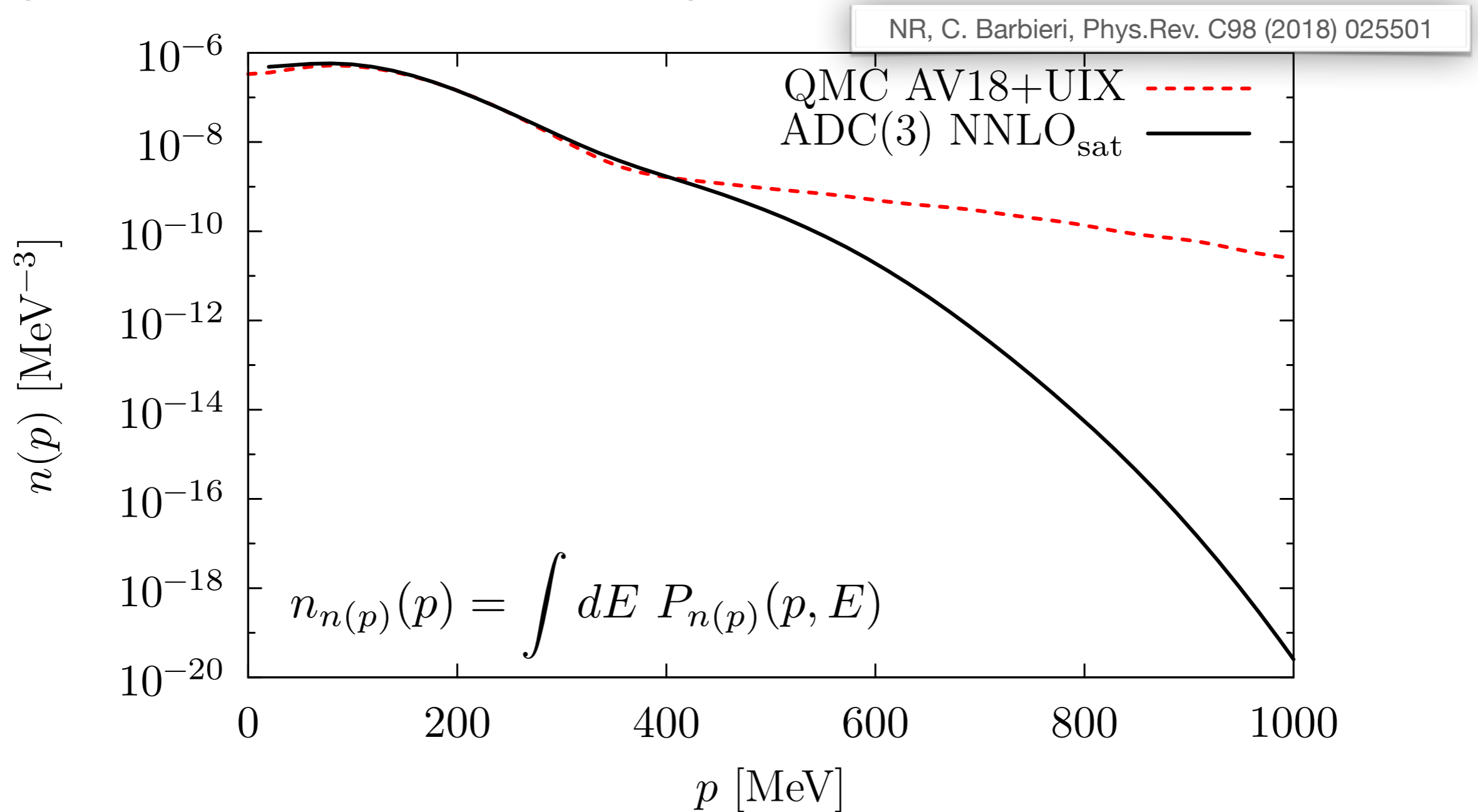
- Single particle momentum distribution of ^{16}O



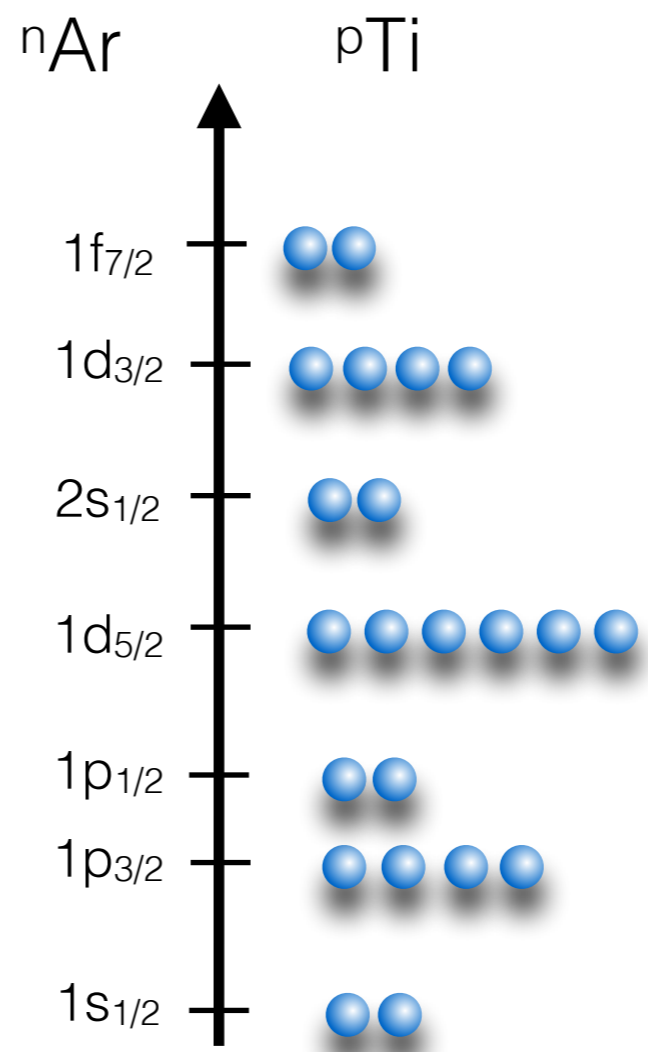
- The momentum distribution reflects the fact that NNLO_{sat} is softer than AV18+UIX.

Benchmark the nuclear model: ^{16}O momentum distribution

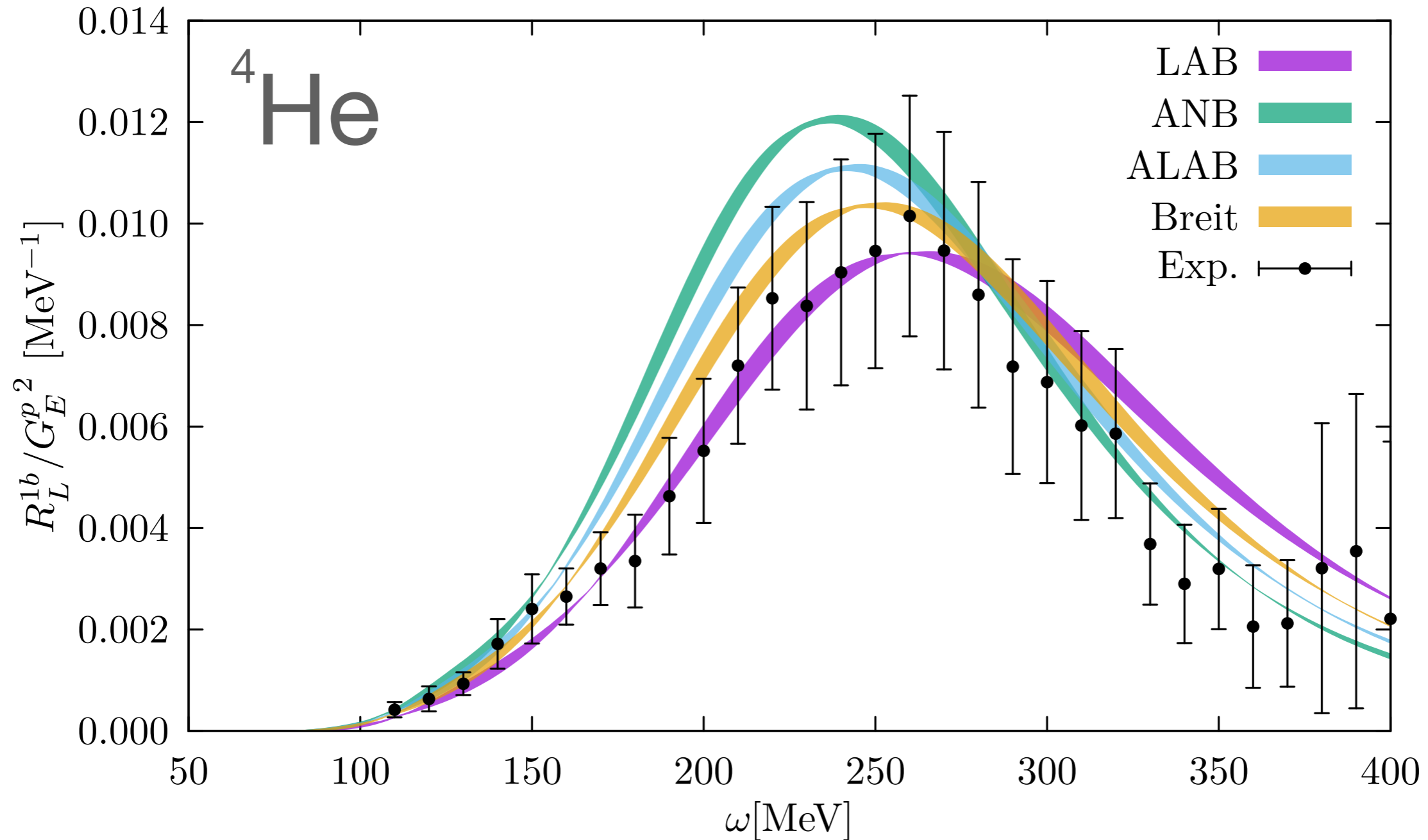
- Single particle momentum distribution of ^{16}O , log scale



- The momentum distribution reflects the fact that NNLO_{sat} is softer than AV18+UIX.



Relativistic effects in a correlated system



- Longitudinal responses of ^4He for $|q|=700$ MeV in the four different reference frames. The curves show differences in both peak positions and heights.

Relativistic effects in a correlated system

- The frame dependence can be drastically reduced if one assumes a two-body breakup model with relativistic kinematics to determine the input to the non relativistic dynamics calculation

$$p^{fr} = \mu \left(\frac{p_N^{fr}}{m_N} - \frac{p_X^{fr}}{M_X} \right) \quad \longleftrightarrow \quad \mu = \frac{m_N M_X}{m_N + M_X}$$

$$P_f^{fr} = p_N^{fr} + p_X^{fr}$$

- The relative momentum is derived in a relativistic fashion

$$\omega^{fr} = E_f^{fr} - E_i^{fr}$$

$$E_f^{fr} = \sqrt{m_N^2 + [\mathbf{p}^{fr} + \mu/M_X \mathbf{P}_f^{fr}]^2} + \sqrt{M_X^2 + [\mathbf{p}^{fr} - \mu/m_N \mathbf{P}_f^{fr}]^2}$$

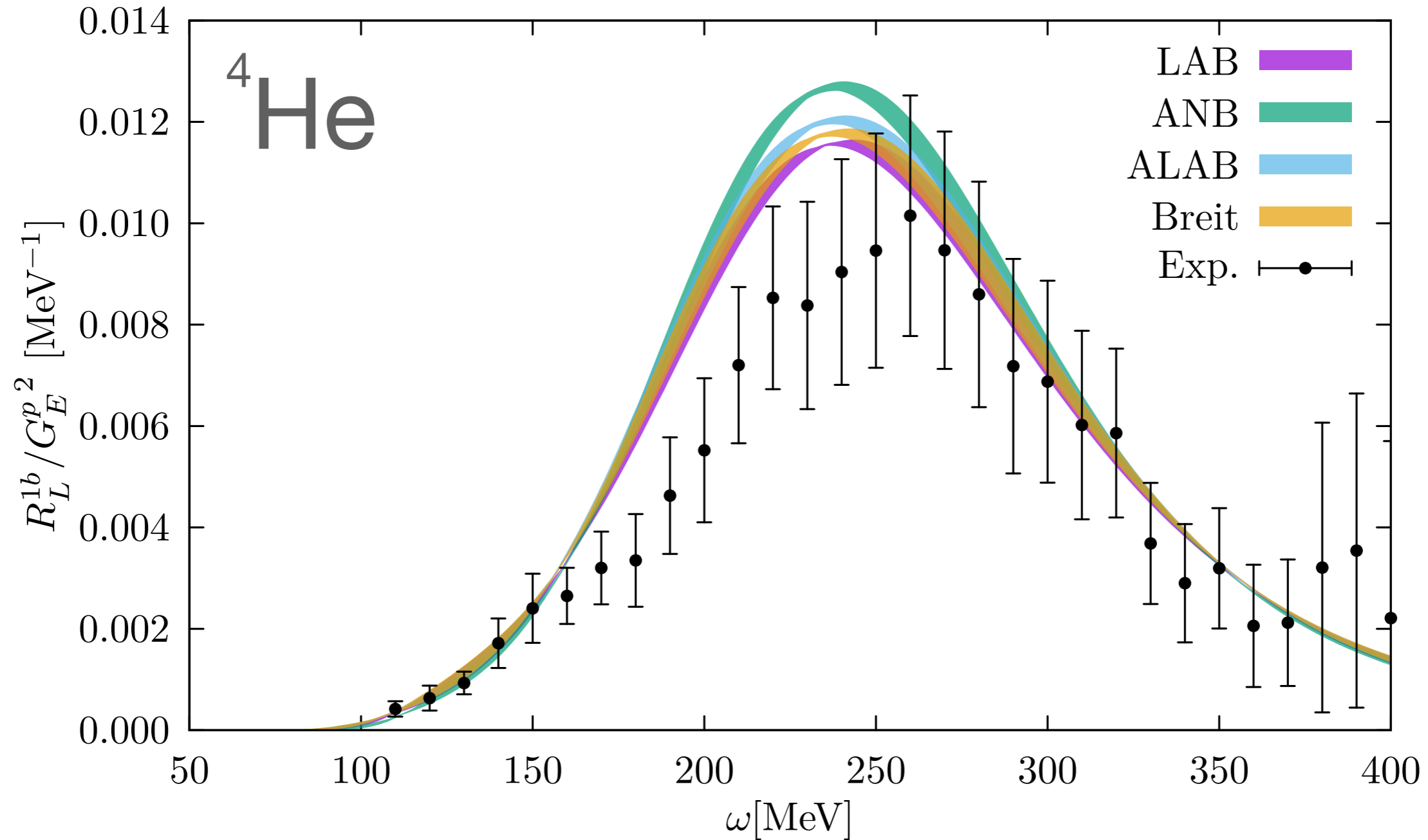
- And it is used as input in the non relativistic kinetic energy

$$e_f^{fr} = (p^{fr})^2 / (2\mu)$$

- The energy-conserving delta function reads

$$\delta(E_f^{fr} - E_i^{fr} - \omega^{fr}) = \delta(F(e_f^{fr}) - \omega^{fr}) = \left(\frac{\partial F^{fr}}{\partial e_f^{fr}} \right)^{-1} \delta[e_f^{fr} - e_f^{rel}(q^{fr}, \omega^f)]$$

Relativistic effects in a correlated system



- Longitudinal responses of ${}^4\text{He}$ for $|q|=700$ MeV in the four different reference frames. The different curves are almost identical.

Extension of the factorization scheme to two-nucleon emission amplitude

$$|X\rangle \longrightarrow |\mathbf{p} \mathbf{p}'\rangle \otimes |n_{(A-2)}\rangle = |n_{(A-2)}; \mathbf{p} \mathbf{p}'\rangle ,$$

We can introduce the two-nucleon Spectral Function...

$$P(\mathbf{k}, \mathbf{k}', E) = \sum_n |\langle n_{(A-2)}; \mathbf{k} \mathbf{k}' | 0 \rangle|^2 \delta(E + E_0 - E_n)$$

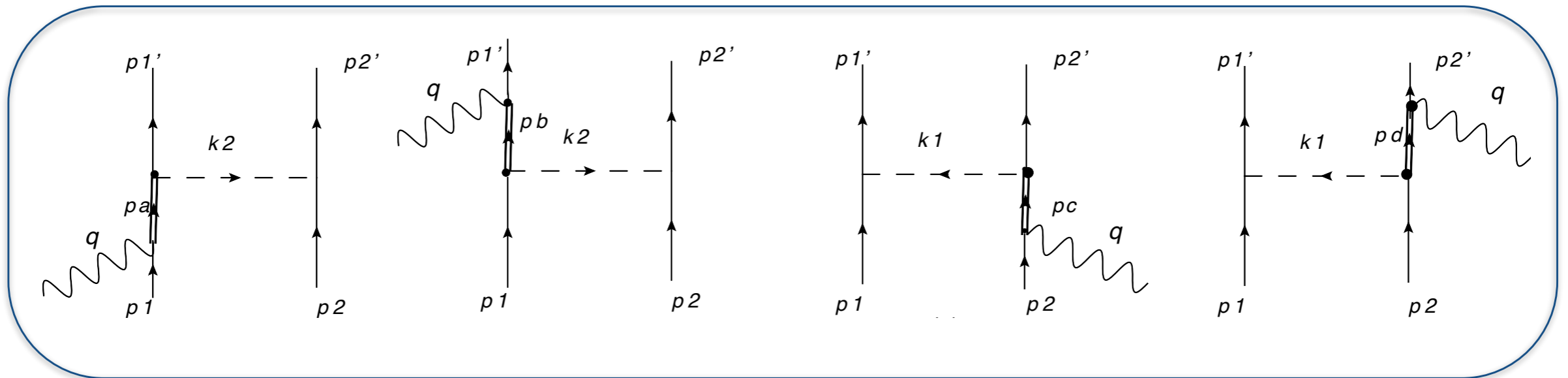
probability of removing two nucleons leaving the A-2 system with energy E

The pure 2-body & the interference contribution to the hadron tensor read

$$W_{2p2h,22}^{\mu\nu} \propto \int d^3k d^3k' d^3p d^3p' \int dE P_{2h}(\mathbf{k}, \mathbf{k}', E) \langle \mathbf{k} \mathbf{k}' | j_{12}^{\mu} | \mathbf{p} \mathbf{p}' \rangle \langle \mathbf{p} \mathbf{p}' | j_{12}^{\nu} | \mathbf{k} \mathbf{k}' \rangle$$

$$W_{2p2h,12}^{\mu\nu} \propto \int d^3k d^3\xi d^3\xi' d^3h d^3h' d^3p d^3p' \phi_{\xi\xi'}^{hh' *} \langle \mathbf{p}, \mathbf{p}' | j_{12}^{\nu} | \xi, \xi' \rangle$$

$$\left[\phi_k^{hh' p'} \langle \mathbf{k} | j_1^{\mu} | \mathbf{p} \rangle + \phi_k^{hh' p} \langle \mathbf{k} | j_2^{\mu} | \mathbf{p}' \rangle \right]$$



The Rarita-Schwinger (RS) expression for the Δ propagator reads

$$S^{\beta\gamma}(p, M_\Delta) = \frac{\not{p} + M_\Delta}{p^2 - M_\Delta^2} \left(g^{\beta\gamma} - \frac{\gamma^\beta \gamma^\gamma}{3} - \frac{2p^\beta p^\gamma}{3M_\Delta^2} - \frac{\gamma^\beta p^\gamma - \gamma^\gamma p^\beta}{3M_\Delta} \right)$$

WARNING

If the condition $p_\Delta^2 > (m_N + m_\pi)^2$ the real resonance mass has to be replaced by $M_\Delta \rightarrow M_\Delta - i\Gamma(s)/2$ where $\Gamma(s) = \frac{(4f_{\pi N\Delta})^2}{12\pi m_\pi^2} \frac{k^3}{\sqrt{s}} (m_N + E_k)$.

Hadronic monopole form factors

$$F_{\pi NN}(k^2) = \frac{\Lambda_\pi^2 - m_\pi^2}{\Lambda_\pi^2 - k^2}$$

$$F_{\pi N\Delta}(k^2) = \frac{\Lambda_{\pi N\Delta}^2}{\Lambda_{\pi N\Delta}^2 - k^2}$$

and the EM ones

$$F_{\gamma NN}(q^2) = \frac{1}{(1 - q^2/\Lambda_D^2)^2},$$

$$F_{\gamma N\Delta}(q^2) = F_{\gamma NN}(q^2) \left(1 - \frac{q^2}{\Lambda_2^2}\right)^{-1/2} \left(1 - \frac{q^2}{\Lambda_3^2}\right)^{-1/2}$$

where $\Lambda_\pi = 1300$ MeV, $\Lambda_{\pi N\Delta} = 1150$ MeV, $\Lambda_D^2 = 0.71\text{GeV}^2$,
 $\Lambda_2 = M + M_\Delta$ and $\Lambda_3^2 = 3.5\text{ GeV}^2$.